Variability in Above and Belowground Carbon Stocks in a Siberian Larch Watershed

Elizabeth E. Webb
Woods Hole Research Center, 149 Woods Hole Road, Falmouth, MA, 02540

Kathryn Heard
Western Washington University, 516 High Street, Bellingham, WA 98225
Bellingham, Washington

Susan M. Natali*
Woods Hole Research Center, 149 Woods Hole Road, Falmouth, MA, 02540

Andrew G. Bunn
Department of Environmental Science, Western Washington University, 516 High Street, Bellingham, WA 98225

Heather D. Alexander
Department of Forestry, Forest and Wildlife Research Center, Mississippi State University, MS 39762

Logan T. Berner
School of Informatics, Computing, and Cyber Systems, Northern Arizona University, Flagstaff, AZ 86011

Alexander Kholodov
University of Alaska, 903 Koyukuk Dr., Fairbanks, AK, 99775
Institute of Physical-Chemical and Biological Problems of Soil Science RAS, 2 Institutskaya str., Pushchino, Russia.

Michael M. Loranty
Department of Geography, Colgate University, 13 Oak Dr, Hamilton, New York 13346

John D. Schade
Woods Hole Research Center, 149 Woods Hole Road, Falmouth, MA, 02540

Valentin Spektor,
Melnikov Permafrost Institute, Siberian Branch of the Russian Academy of Sciences, Yakutsk, Siberia

Nikita Zimov
Northeast Science Station, Cherskiy, Russia

*Corresponding author. Please direct correspondence to snatali@whrc.org

ABSTRACT

Permafrost soils store between 1,330-1,580 Pg carbon (C), which is three times the amount of C in global vegetation, almost twice the amount of C in the atmosphere, and half of the global soil organic C pool. Despite the massive amount of C in permafrost, estimates of soil C storage in the high latitude permafrost region are highly uncertain, primarily due to under sampling at all spatial scales; circumpolar soil C estimates lack sufficient continental spatial diversity, regional intensity, and replication at the field-site level. Siberian forests are particularly under sampled, yet the larch forests that dominate this region may store more than twice as much soil C as all other boreal forest types in the continuous permafrost zone combined. Here we present above and belowground C stocks from twenty sites representing a gradient of stand age and structure in a larch watershed of the Kolyma River, near Cherskiy, Sakha Republic, Russia. We found that the majority of C stored in the top 1 m of the watershed was stored belowground (92%), with 19% in the top 10 cm of soil and 40% in the top 30 cm. Carbon was more variable in surface soils (10 cm; coefficient of variation (CV) = 0.35 between stands) than in the top 30 cm (CV=0.14) or soil profile to 1 m (CV=0.20). Combined active layer and deep frozen deposits (surface - 15 m) contained 205 kg C m^{-2} (yedoma, non-ice wedge) and 331 kg C m^{-2} (alas), which, even when accounting for landscape-level ice content, is an order of magnitude more C than that stored in the top meter of soil and two orders of magnitude more C than in aboveground biomass. Aboveground biomass was composed of primarily larch (53%) but also included understory vegetation (30%), woody debris (11%) and snag (6%) biomass. While aboveground biomass contained relatively little (8%) of the C stocks in the watershed, aboveground processes were linked to thaw depth and belowground C storage. Thaw depth was negatively related to stand age, and soil C density (top 10 cm) was positively related to soil

moisture and negatively related to moss and lichen cover. These results suggest that as the climate warms, changes in stand age and structure may be as important as direct climate effects on belowground environmental conditions and permafrost C vulnerability.

1 INTRODUCTION

Boreal forests cover roughly 22% of the earth's terrestrial landscape (Chapin et al., 2000) and account for approximately 9% of the global vegetation carbon (C) stock (Carvalhais et al., 2014). Most of the C in boreal forests, however, is stored in the soil (Pan et al., 2011), where cold and wet conditions have limited microbial decomposition, and as a result, C has accumulated over the past several millennia (Hobbie et al., 2000; Trumbore and Harden, 1997). Recent estimates suggest that continuous and discontinuous permafrost in the boreal region store around 137 Pg, or 40% of near surface permafrost (< 1 m) C (Loranty et al., 2016). Despite the massive amount of C present in the boreal region, the quantity of C stored here and the magnitude of the change in C stocks that will result from climate change is one of the least understood carbon-climate feedbacks (Schuur et al., 2015).

Over the past fifty years, air temperatures in the Arctic have risen nearly twice the global average as a result of climate change (Christensen et al., 2013), and this accelerated rate of warming means that the vast amount of C stored in high latitude systems is vulnerable to loss to the atmosphere (Koven et al., 2015; Schuur et al., 2015). The amount of C released as a result of thaw will be highly dependent on concurrent changes in topography and hydrology (Liljedahl et al., 2016; Schneider Von Deimling et al., 2015), vegetation (Guay et al., 2014; Sturm et al., 2005) fire regimes (Berner et al., 2012; Kasischke and Turetsky, 2006; Rogers et al., 2015; Soja et al., 2007), nutrient availability (Mack et al., 2004; Salmon et al., 2016), and as soil organic C lability (Harden et al., 2012; Schädel et al., 2014). Yet despite the vulnerability of permafrost soils to increased thaw and C release due to climate change, there is a lack of data quantifying the C stocks in northern latitudes compared to other regions.

Permafrost C pool estimates tend to be dominated by sites located in Alaska or western Russia, with very few data points from the Russian low Arctic or Canadian high Arctic (Hugelius et al., 2014; Tarnocai et al., 2009). As a result, many regions are under-represented in circumpolar permafrost C estimates (Hugelius et al., 2014; Johnson et al., 2011; Mishra et al., 2013; Tarnocai et al., 2009). Even in Alaska, which is one of the most densely sampled Arctic sub-regions, Mishra and Riley (2012) found that the current sample distribution is insufficient to characterize regional soil organic C (SOC) stocks fully because of SOC variation across vegetation types, topography, and parent material. Furthermore, permafrost regions are characterized by high heterogeneity in soil C stocks due to variability in soil-forming factors (Vitharana et al., 2017) and at small spatial scales due to cryogenic processes (i.e., cryoturbation at the sub-meter scale). As a result, sampling at higher spatial resolution may provide more accurate estimates of soil C stocks (Johnson et al., 2011; Tarnocai et al., 2009). Therefore, understanding variation in soil properties at the meter scale is critical for reducing uncertainty in estimates of current and future permafrost C pools (Beer, 2016).

Pleistocene-aged, C and ice rich permafrost (i.e. yedoma) deposits occur across Siberia and Alaska (Strauss et al., 2013) and are particularly important for regional soil C estimates. Yedoma deposits froze relatively quickly in geologic history (Schirrmeister et al., 2011; Zimov et al., 2006), and as a consequence, these deep deposits (on average 25 m; Zimov et al. 2006) are C rich compared to some other permafrost soils (Strauss et al., 2013; Zimov et al., 2006). Approximately 30% of high latitude permafrost C is found in these yedoma deposits, even though they comprise only 7% of the landscape (Walter Anthony et al., 2014). However, due to limited sampling of deep (> 3 m) permafrost, establishing how much C is in these deposits is

72 difficult, leading to high uncertainty in estimates of soil C pools in yedoma deposits (Strauss et
73 al., 2013; Walter Anthony et al., 2014).
74 While vegetation stores a relatively small portion of the C pool in boreal forests
75 (approximately 20%; Pan et al., 2011), it plays a crucial role in local and global C cycling, and
76 many future changes in C fluxes in this biome will likely occur as a result of changes in
77 vegetation (Elmendorf et al., 2012; Euskirchen et al., 2009; Myers-Smith et al., 2015; Swann et
78 al., 2010). With increased temperatures, boreal forests are susceptible to insect invasions (Berg
79 et al., 2006; Kurz et al., 2008), moisture stress (Beck et al., 2011; Trahan and Schubert, 2016;
80 Walker et al., 2015), tree line advance and retrogression (Lloyd, 2005; Pearson et al., 2013), and
81 more frequent forest fires (Kasischke and Turetsky, 2006; Rogers et al., 2015; Soja et al., 2007),
82 which all have the potential to alter C cycling significantly in the region. Importantly, climate-
83 change driven alterations in forest cover, composition, and structure will influence regional
84 energy balance through impacts on surface albedo, evapotranspiration, and ground insulation,
85 which will in turn affect ground thaw and soil C cycling (Chapin et al., 2005; Euskirchen et al.,
86 2009; Fisher et al., 2016; Jean and Payette, 2014; Loranty et al., 2014).
87 However, the aboveground processes that regulate C dynamics are not homogenous
88 throughout the boreal biome (Goetz et al., 2007). For example, the fire regimes of larch (*Larix*
89 *spp.*) and pine (*Pinus sylvestris)* forests in Siberia are typically dominated by low to medium
90 intensity fires whereas dark coniferous forests common in Alaska and Canada are characterized
91 by higher intensity and severity fires (Rogers et al., 2015; Soja et al., 2006, 2007; Tautenhahn et
92 al., 2016). The dynamics of larch forests are particularly important, as they store more than
93 twice the amount of SOC of all other boreal forest types in the continuous permafrost zone
94 combined (Loranty et al., 2016). Despite this, larch forests in Siberia are notably under studied;

indeed, the estimate of C stored in Russian forests is the least well constrained of all forest systems globally (Shuman et al., 2013).

In this study, we aim to reduce the uncertainty of regional C estimates by providing a comprehensive assessment of vegetation, active layer, and permafrost C stocks in the Kolyma River watershed in Northeast Siberia, Russia. We present aboveground and belowground (to 1 m) C stocks from data collected from 20 sites across the watershed along with deep permafrost C pools to 15 m depth from a yedoma deposit and an alas (thermokarst depression). We compare variation in soil C pools at meter to kilometer scales in order to quantify the variability of permafrost C at small spatial scales. Additionally, we examine the drivers of thaw depth and C density of active layer soils to understand environmental controls over these variables across the watershed. Together, these analyses allow us to estimate C pools and controls over changes in these pools that will likely occur with climate change.

2 METHODS

2.1 Site description

Our study area was a watershed ('Y4 watershed', ~3 km^2; Figure 1) located within the Kolyma River basin, which is the largest river basin (650,000 km^2) completely underlain by continuous permafrost (Holmes et al., 2012). The Y4 watershed is located near Cherskiy, Sakha Republic, Russia approximately 130 km south of the Arctic Ocean and is underlain by yedoma, which is widespread across the region (Grosse et al., 2013). The climate is continental with short, warm summers (Jul avg: 12 °C) and long, cold winters (Jan avg: -33 °C). Annual precipitation is low (~230 mm) and often occurs during summer (Cherskiy Meteorological Station; S. Davydov,

117 unpub data). Mean summer temperatures in this region increased by 1°C from 1938 to 2009
118 (Berner et al., 2013).
119 There are two main types of cryogenic deposits within the watershed. Upland areas are
120 Late Pleistocene syngenetic ice rich deposits of yedoma. Drained thaw lake depressions are
121 underlain by alas consisting of lacustrine-wetland sediments in the upper pedon and taberal (i.e.
122 yedoma that thawed in a talik) deposits in the lower part of the profile. Permafrost temperatures
123 at 15 m vary from -2.8°C at the hilltops with relatively thin organic layers to -4°C in thermokarst
124 depressions with thick (up to 20 cm) moss and peat layers (A. Kholodov, unpub data).
125 Forests in the watershed are composed of a single larch species, *Larix cajanderi*, with a
126 well-developed understory of deciduous shrubs (primarily *Betula nana*, *Salix* spp., and
127 *Vaccinium uliginosum*), evergreen shrubs (e.g. *Vaccinium vitis-idaea, Empetrum nigrum,*
128 *Rhododendron subarcticum*), forbs (e.g., *Equisetum scirpoides, Pyrola* spp., and *Valeriana*
129 *capitate*), graminoids (*Calamagrostis* spp.), moss (e.g. *Aulacomnium palustre, Dicranum* spp.,
130 and *Polytrichum* spp), and lichen (e.g. *Cladonia* spp, *Peltigera aphthosa,* and *Flavocetraria*
131 *cucullata*).
132
133 **2.2 Site selection and sampling design**
134 We selected 20 stands (i.e. 'sites') in the Y4 watershed that spanned a range of tree
135 aboveground biomass, as inferred from tree shadows mapped using high-resolution (50 cm)
136 WorldView-1 satellite imagery (Berner et al., 2012; Figure 1). All sites were located in forested
137 stands except for one in a *Salix*-dominated riparian zone (Site 17) and another in a *Sphagnum*-
138 dominated alas (Site 18; Table 1). Within each site, we established three 20 m long by 2 m wide
139 plots, each of which was separated by 8 m and ran parallel to slope contours (Figure S1). In the

absence of a discernable slope, transects were aligned north-south. All sampling was conducted in July 2012 and 2013 except stand age, which was sampled in 2016.

2.3 Stand Age

To determine stand age, we collected a wood slab or core from the base (~ 30 cm above the organic layer) of 5-10 trees sampled randomly within each stand. Wood samples were dried at 60 °C and then sanded sequentially with finer grit sizes to obtain a smooth surface. Each sample was then scanned and the annual growth rings were counted using WinDendro (Regent Instruments, Inc., Ontario).

2.4 Solar Insolation and Slope

Slope and aspect at each site were determined from a 4-m-resolution digital elevation model of the watershed created by the Polar Geospatial Center (http://www.pgc.umn.edu/) using stereo-pairs of World ViewX imagery. Solar insolation was estimated using the Solar Radiation analyses toolset in ArcGIS version 10 (ESRI , Redlands, CA). The toolset used variability in the orientation (slope and aspect) to calculate direct and diffuse radiation for each pixel of the elevation model in the Y4 watershed using viewshed algorithms (Fu and Rich, 2002; Rich et al., 1994). We report total insolation on the summer solstice for each pixel.

2.5 Aboveground biomass

We measured diameter at breast height (DBH; 1.4 m height) or basal diameter (BD; < 1.4 m height) of all trees and snags (i.e., dead trees standing ≥ 45° to the forest floor) within each 40-m^2 plot (n= 3/site). Live and dead aboveground tree biomass were determined based on

allometric equations developed from *L. cajanderi* trees harvested near Cherskiy (Alexander et al., 2012). Tree biomass was converted to C mass using a C concentration of 46% C for foliage (live trees only), 47% C for stemwood/bark and snag, and 48% C for branches (Alexander et al., 2012).

We estimated understory percent cover in six 1-m^2 subplots at each site; subplots were placed at both ends of each of the three plots (at 0 and 20 m; Figure S1). Understory vegetation was sorted into functional types, which included shrub (evergreen and deciduous), herbs (forb and graminoids), moss, lichen, and other (litter, woody debris and bare ground). In each site, understory vascular plant biomass was determined in three 0.25 m^2 quadrats, each of which was located within one of the percent cover plots. We measured basal diameter of tall deciduous shrubs (*Alnus* spp., *B. nana*, and *Salix* spp.) and used published allometric relationships to derive biomass (Berner et al., 2015). All remaining vascular plants were harvested and dried at 60 ºC for 48 hours for dry mass determination. We converted live understory biomass values to C pools by multiplying biomass by 48% C content.

Following the line-intercept method for measuring woody debris (Brown, 1974), we set a 20-m transect along the middle of each plot, and counted the number of times woody debris intercepted the transect for Class I fine woody debris (FWD; 0.0-0.49 cm diameter) and Class II FWD (0.5-0.99 cm) along the first 2 m, Class III FWD (1.0 – 2.99cm) along the first 10 m, and classes IV FWD (3.0-4.99 cm), V FWD (5.0-6.99 cm), and downed coarse woody debris (CWD; > 7 cm diameter) along the entire 20 m length. We calculated the mass of woody debris according to Alexander et al. (2012) using previously published multipliers for softwood boreal trees from the Northwest Territories of Canada for FWD (Nalder et al., 1997) and decay class and density values for softwood boreal tree species within Ontario, Canada for CWD (Ter-

186 Mikaelian et al., 2008). Mass values were converted to C pools based on average C
187 concentration of *L. cajanderi* boles (47% C). Total aboveground biomass (AGB) is reported as
188 the sum of the C pools in woody debris, snags, trees, and understory biomass.
189
190 **2.6 Canopy cover and leaf area index**
191 We measured canopy cover under uniform, diffuse light conditions at the center of each
192 site in four cardinal directions using a convex spherical densitometer, and Leaf Area Index (LAI)
193 using both hemispherical photography and an LAI-2000 Plant Canopy Analyzer (Li-COR,
194 Nebraska, NE, USA). The LAI-2000 was placed ~1 m above the ground at the center of each
195 site, and LAI estimates were divided by a factor of 0.68 (Chen et al., 2005) to account for foliage
196 clumping (Chen et al., 1997). Hemispherical photographs were taken ~1 m off the ground using
197 a Sigma SD 15 digital reflex camera with Sigma 4.5 mm F2.8 EX DC circular fisheye lens. A
198 N-S reflector was used for N orientation, and photographs were taken using automatic settings at
199 the center of each of the three transects at each site. The hemispherical photographs were
200 analyzed using Hemiview software.
201
202 **2.7 Thaw depth/organic layer depth**
203 We measured thaw depth using a metal thaw probe every meter along a 20 m transect
204 placed along the center of each plot (measured from 9 July through 3 August; does not represent
205 maximum thaw). Organic layer depth (OLD) was measured at 5 m intervals along each transect
206 by cutting through the active layer soil with a serrated knife and visually identifying and
207 measuring the depth to the organic-mineral boundary.
208

209 **2.8 Soil sampling and analysis**

210 Active layer soils were collected from all sites. Surface permafrost soils (approximately
211 the top 60 cm of frozen soil, which contained some frozen active layer soil) were sampled at
212 seven sites (3 cores per site), and deep permafrost (15 m depth) was sampled at two sites (Sites
213 18 and 19). We collected six active layer samples from each site, one at each end of the 20-m-
214 long plots. We used a serrated knife to collect an 8 cm x 8 cm sample from the organic layer,
215 and a 2 cm diameter manual corer to collect the top 10 cm of mineral soil. When less than 5 cm
216 of mineral soil was thawed at the time of sampling, the mineral soil sample was excluded from
217 analysis (n=5). At the seven sites where surface permafrost was sampled, we collected mineral
218 soil to frozen ground (average 28 cm thawed mineral soil depth) using a manual corer, and
219 sampled approximately 60 cm depth of frozen soil with a Soil Ice and Permafrost Research
220 Experiment (SIPRE) auger (7.62 cm diameter). We collected two deep permafrost cores with a
221 rotary drill rig (UKB-12/25, Drilling Technology Factory); one deep core was collected from a
222 site underlain by yedoma and the other from an alas. Carbon pools presented for deep permafrost
223 include C in the active layer sampled at the drilling location. Carbon pools reported for 1 m
224 depth were calculated using the seven surface permafrost samples as well as the top 1 m of the
225 deep core from the yedoma site. All permafrost samples were kept frozen until analyzed as
226 described below.

227 Surface permafrost cores were sectioned into 10 cm increments. Coarse-roots (> 2 mm)
228 were removed from all active layer and surface permafrost soils, and fine roots and organic soils
229 were dried at 60 °C for 48 hours while mineral soils were dried at 105 °C for at least 48 hours.
230 Gravimetric water content (GWC) was determined as the ratio of soil water mass to soil dry
231 mass, and was reported as a percentage (i.e., GWC x 100). Organic matter content was

232 measured as the percent mass lost from dried soil after combusting for 4 hours at 450°C. Soil C
233 content was analyzed on a subset of soils (35 of 111 organic soils; 119 of 271 active layer and
234 surface permafrost mineral soil; and 30 of 149 deep permafrost samples) on a Costech CHN
235 analyzer at St. Olaf College or at the University of Georgia Stable Isotope Ecology Lab. Carbon
236 concentrations of the full set of soil samples were then modeled using a linear relationship
237 between organic matter content and %C (C% = 0.524 * OM% – 0.575; R^2=0.96 for active layer
238 and surface permafrost; C% = 0.391 * OM% – 0.103; R^2=0.86 for deep permafrost samples).
239 Carbon content of coarse roots was assumed to be 50%. Sampled soils were reclassified as
240 organic or mineral as needed (< 1% of samples) based on soil C content (C ≥ 20% for organic
241 soils).
242 Bulk density (BD) was determined as the mass of dry soil per unit volume (g cm^{-3}).
243 Volume of active layer soil samples was determined by measuring the ground area and depth
244 from where the soil sample was removed. Volume of permafrost samples was quantified by
245 water displacement. Ice volume was determined based on soil water content and assuming an ice
246 density of 0.9167 g cm^{-3}.
247 Soil C stocks in each depth increment were calculated as the product of %C, BD and soil
248 depth. For the deep permafrost samples, sub-samples used for %C, %OM, and BD
249 measurements were collected from adjacent depth increments; therefore, for the %C-%OM
250 regression and C pool calculations, we used adjacent depth increments or interpolated values
251 between two adjacent depths.
252
253 **2.9 Statistical analysis**

To compare the variance in soil C among sites and studies, we used the coefficient of variation (CV), which is the ratio of the standard deviation to the mean. The CV is independent of the unit or magnitude and can be used to compare intra-site variation (how variable the data are relative to the mean value) among sites even if the mean of the sites is vastly different. We also used percent variation, which was calculated by subtracting the minimum value from the maximum value and dividing by the maximum value.

We used a linear model to determine the relationship between canopy cover and LAI and larch biomass and the relationship between the different components of AGB. To determine potential environmental drivers of thaw depth and soil C, we fit a mixed effects linear model using the nlme package in R (Pinherio et al., 2013), using average plot-level data (3/site) as a replicate for each site. The fixed effects were the environmental variables, and the random effect was the nested study design (plots within sites). Both thaw depth and soil C were log-transformed to meet the assumption of normality. After collinear explanatory variables were removed from analysis using a variance inflation factor of three (as suggested by Zuur et al. (2009)), we considered densiometry, organic layer depth, stand age, live shrub biomass, woody debris, tree density, snag density, summer insolation, percent herbaceous cover, percent moss cover, percent lichen cover, percent other cover, soil C, BD, and root C, as explanatory variables for the thaw depth model. For the soil C model the environmental variables considered were: slope, summer insolation, snag biomass, live tree biomass, live shrub biomass, woody debris, tree density, percent herbaceous cover, percent moss cover, percent lichen cover, percent other cover, thaw depth, organic layer depth, root carbon, and moisture. The best model for each analysis was selected using backwards stepwise reduction of variables to obtain the lowest

Akaike information criterion (AIC) and the residuals of all final models were checked for normality and homogeneity of variance (Burnham and Anderson, 2002).

All reported errors are the standard error of the mean. All statistical analyses were conducted using the statistical program R (R Core Development Team, 2012).

3 RESULTS

3.1 Distribution of carbon pools

The majority of C in the watershed to 1 m depth was stored belowground (92%; 10.9 ± 0.8 kg C m^{-2} in top 1 m; Figure 2), with 19% in the top 10 cm of soil and 40% in the top 30 cm. The top 10 cm of soil alone contained 58% more C than the total aboveground C stocks.

3.2 Stand density, stand age, and aboveground biomass

Stand density in the watershed ranged from 0.01 to 0.43 trees m^{-2} in the forested sites (mean density was 0.07 ± 0.02 trees m^{-2}; Table 2). Mean stand age was 150 (±17) yrs (Table 1), but there was a large range in tree ages among sites (23-221 yrs) and within sites (average range: 78 yrs; maximum range: 238 yrs; minimum range: 7 yrs; Table S1).

Total C in AGB averaged 959 ± 150 g C m^{-2} across sites in the watershed, with 53% in larch biomass (460 ± 77 g C m^{-2}), 30% in understory biomass (254 ± 28 g C m^{-2}) 11% in woody debris (94 ± 16.5 g C m^{-2}), and 6% in standing dead tree mass (55 ± 19 g C m^{-2}) (Figure 2; Table 3). Among sites across the watershed, aboveground C varied up to 95%. Together, all C in AGB contributed 8% to the total amount of C stored above and belowground (to 1 m) across the watershed. Mean stand age was positively related to mean stand AGB R^2=0.21, $p<0.001$ and negatively related to mean stand thaw depth (R^2=0.58, $p<0.001$).

299 Larch aboveground biomass was also highly variable across the watershed, with some
300 sites as low as 0 or 1.7 g C m^{-2} and others as high as 1,340 and 1,362 g C m^{-2}. Of the three
301 techniques used for estimating canopy cover, LAI values from hemispherical photography (Table
302 2) showed the highest correlation with larch biomass (R^2= 0.69, p <0.001), but larch biomass
303 was also significantly associated with canopy density (R^2= 0.5, p< 0.001). There was no
304 relationship between larch biomass and understory biomass (p = 0.4); however, the percent cover
305 of tall shrubs was negatively related to both moss (R^2=0.2, p<0.001) and lichen cover (R^2=0.2,
306 p<0.001).

307 **3.3 Surface soils**

308 Average C content of the organic horizon was 37.6 (± 0.8) %C, whereas C content of the
309 thawed mineral horizon (0-10 cm) was 4.6 (± 0.48) %C. There were 2.24 (± 1.22) kg C m^{-2}
310 stored in the organic layer (average organic layer depth=11.2 ± 0.2 cm) and 1.96 (± 0.07) kg C
311 m^{-2} in the top 10 cm of the mineral layer (Table 4).

312 There was large variation in BD, soil moisture (GWC), soil C content and thaw depth
313 among sites (Table 5). Carbon content and GWC were more variable in mineral soils than in
314 organic ($CV_{mineral}$ = 0.55 for %C and 0.48 for GWC; $CV_{organic}$ = 0.15 for %C and 0.36 for GWC),
315 while BD was more variable in organic soils ($CV_{organic}$ = 0.51; $CV_{mineral}$ = 0.3). While the CV of
316 thaw depth was not particularly high (0.28), the difference between the sites with the highest and
317 lowest thaw depth measured was still 65%, underscoring the heterogeneity of soil properties
318 across the watershed. Variation in thaw depth was primarily due to stand age (Figure 3; Table
319 S2).

320 Soil C density in the top 10 cm of the ground surface (i.e., 0-10 cm soil depth, which may
321 have contained both organic and mineral soils) varied up to 93% across the watershed (range:

322 0.51-7.14 kg C m^{-2}; Table 4; Table S2), but the coefficient of variation (CV) was larger within
323 sites (0.32) than it was between sites (0.26), indicating that soil C is more variable at the meter
324 scale than it is at the kilometer scale. The distribution of soil C density in the top 10 cm was best
325 explained by soil moisture, percent moss, and percent lichen cover (Table S2); soil C density was
326 positively related to soil moisture and negatively related to percent moss and lichen cover
327 (Figure 4).

328 Soil in the top 30 cm of the profile contained on average 4.8 ± 0.3 kg C m^{-2}, but soil C
329 density in the top 30 cm varied by 56% across the watershed as a whole. The average CV within
330 a site was 0.16 whereas the CV among sites was 0.22, indicating C density at 30 cm is similar or
331 more variable across the watershed than at the meter scale. The top 1 m of soil contained 10.9 ±
332 0.8 kg C m^{-2}(13.8 ± 3.0 kg C m^{-2} with alas site; Table S4). Soil C in the top 1 m varied by 63%
333 across the watershed and by 44% among sites. The average CV within a site was 0.15 whereas
334 among sites the CV was 0.20, indicating soil C to 1 m is similarly variable at the meter and
335 kilometer scales. Ice content in the top 1 m was on average 68 ± 2% by volume, with a range of
336 between 51% and 80%.

337 **3.5 Deep permafrost soils**

338 Deep permafrost soils (includes surface active layer to 15 m) contained 205 kg C m^{-2} (site
339 19; yedoma deposit, non-ice wedge) and 331 kg C m^{-2} (site 18; alas). Carbon density at each 1
340 m interval ranged from 7.87-21.63 kg C m^{-3} in the yedoma deposit and 6.9-14.5 kg C m^{-3} in the
341 deeper portion of the alas (Figure 5; Table S5). The top 2 m of the alas were characterized by
342 particularly high C density (~30 kg m^{-3}).

343 Highlighting the variability of C in deep permafrost, the total soil C density in the two
344 cores varied by 38%. The alas site had higher GWC than the yedoma site in the first 2 m (GWC:

385 ± 81% and 41 ± 8 %, respectively). Throughout the entire profile, GWC was 46 ± 2% in the yedoma core and 100 ± 23% in the alas core. Overall, BD was similar between the two cores, and most of the variation in BD occurred in the top 5 m (Figure 5).

4 DISCUSSION

4.1 Aboveground biomass

Aboveground C pools within the Y4 watershed represented only a small fraction (8%) of total C pools, likely due to low tree density at most sites (< 0.09 trees m^{-2} in all but one site) and/or young stand ages at a few sites. Low-density, mature (> 75 years old) stands with no recent fire activity are common in this region (Berner et al. 2012); however, wildfires can produce stands of considerably higher density (> 3 trees m^{-2}), which can substantially increase AGB and contribution to total C pools as stands mature (Alexander et al. 2012). Aboveground C pools were similar to those reported by Alexander et al. (2012) for 17 nearby stands of similar age and density, but C in larch AGB was lower (~23%) than a landscape-level estimate (~ 600 g C m^{-2}) across the Kolyma River basin (Berner et al. 2012). Our estimate for C stored in larch AGB was also four times lower than that of a mature (155-yr old), mid-density (0.19 trees m^{-2}) stand near Cherskiy and two times lower than a mature, low-density (0.08 trees m^{-2}) stand near Oymyakon, south of Cherskiy (Kajimoto et al., 2006). In addition, our larch AGB estimates fell within the low range of larch stands across other high-latitude (> 64° N) regions and were generally 3-10 times lower than other stands (Kajimoto et al., 2010). Our considerably lower estimates reflect both the sparse, open grown structure of our stands (Osawa and Kajimoto, 2010) and the poor soil environment (e.g., shallow rooting zone, low soil temperature, low N availability) found in stands near latitudinal and altitudinal treeline (Kajimoto et al. 2010).

Despite the small contribution of AGB to total C pools across our stands, aboveground vegetation composition and structure were important factors related to soil C pools and permafrost thaw (see below). In addition, characteristics of aboveground vegetation are major determinants of land-atmosphere C fluxes (Bradshaw and Warkentin, 2015) and thus remain essential components of C dynamics even when pools are relatively low.

4.2 Variability of soil C pools

Soil C density is controlled by numerous biogeophysical factors such as climate, local geomorphology, soil parent material, time since last disturbance, and vegetation type, all of which lead to high variability in soil C pools at the regional and local scale. Our soil C pool estimates for a Siberian larch forest watershed fall within the range of published assessments that characterize this area (Alexander et al. 2012; Broderick et al. 2015), but are at the low end of other studies (Alexeyev and Birdsey, 1998; Hugelius et al., 2014; Matsuura et al., 2005; Palmtag et al., 2015; Stolbovoi, 2006). For example, our mean estimate of 4.8 ±1 kg C m^{-2} in the top 30 cm of soil is less than half of a published assessment of C stored in soils across Russian larch forests (10.2 kg C m^{-2}; Stolbovoi, 2006), and less than one third of the mean estimate for Turbel soils across the permafrost region (14.7 kg C m^{-2}; Hugelius et al., 2014); however, variation in the permafrost region Turbel soil C pool is high (CV = 0.85; Hugelius et al., 2014), and our mean estimate falls within one standard deviation of this regional mean.

Within larch forests, there is substantial variation in soil C pools at regional scales, driven by variation in soil parent material and climate. For example, larch forests in Northeastern Siberia store significantly more C (16 kg C m^{-2}) in the active layer and have more variable soil C pool estimates than larch forests in Central Siberia (6.3 kg C m^{-2}) (Matsuura and Hirobe, 2010). There is also considerable variation in soil C pools within larch forests at smaller spatial scales.

391 Indeed, the active layer in larch forests located within 50 km from our study site contained twice
392 as much C as found in our study (4.8 ± 0.3 kg C m^{-2} to 30 cm); there was 8.3 kg C m^{-2} in the
393 active layer (38 cm) of a larch forest 44 km from the Y4 watershed (Matsuura et al., 2005) and
394 9.5 ± 2.9 (SD) kg C m^{-2} in the top 30 cm of soils from a forest 3 km away (Palmtag et al., 2015).
395 This variation in soil C pools points to the extreme variability in soil C throughout the landscape,
396 even at the kilometer scale. It also highlights the importance of sampling replication at small
397 scales; with 21 total soil cores at seven sites, our CV (0.13) was less than half of other studies
398 with lower site-level replication (Palmtag et al., 2015).
399 As the climate warms, C in surface permafrost is becoming increasingly vulnerable to
400 thawing and subsequent decomposition and loss to the atmosphere. As such, estimating
401 variation in C pool size is critical for understanding permafrost climate feedbacks. The C stored
402 in the top 1 m of Y4 soils (10.9 ± 0.8 kg C m^{-2}) was similar to the average 1-m C pool reported
403 for the Yakutia region, which comprises a range of ecosystem types (8.1 kg C m^{-2}; Alexeyev and
404 Birdsey, 1998) but 37% lower than the 1 m soil C pool reported in a forest only 3 km away (17.3
405 ± 5.7 kg C m^{-2}; Palmtag et al., 2015). However, the percent difference between our estimate and
406 the nearby study (37%) was similar to the percent difference found between sites in the Y4
407 watershed (44%; Table 4), suggesting that these differences among studies are likely due to
408 natural variation in the landscape.
409 Carbon pool estimates from deep permafrost (>3 m) are limited across the Arctic
410 (Hugelius et al., 2014; Schuur et al., 2015; Tarnocai et al., 2009), yet these data are critical for
411 assessing variation in and controls on C density of yedoma, as these soils have particularly high
412 C density at depth (Strauss et al., 2013; Zimov et al., 2006). The average carbon density of deep
413 permafrost from yedoma deposits in the Y4 watershed (13.5 kg C m^{-3}) was similar to values

reported for yedoma in pan-Arctic summary studies (10 +7/-6 kg C m^{-3}, Strauss et al. (2013); 13.0 ± 0.75 kg C m^{-3} after correction for ice volume, Walter Anthony et al. (2014)) and in taiga sites within 100 km of Cherskiy (12.3-15.4 kg C m^{-3} after correction for ice volume, Walter Anthony et al. (2014) and references therein; 14.3 kg C m^{-3}, Shmelev et al., 2017). Carbon density was almost twice as high in the alas, which is consistent with findings indicating that alas and thermokarst soils store substantially more C (~ 40-70%; Walter Anthony et al. (2014); Strauss et al. (2013); Siewert et al. (2010)) than undisturbed yedoma, a difference that is likely due to higher rates of recent (Holocene) C accumulation at the alas site (Walter Anthony et al., 2014). Yedoma is characterized by high landscape-level ice content due to the prevalence of large ice wedges, which can comprise 31 to 63% of ground volume (Ulrich et al., 2014). Accounting for these deep ice deposits, which were not sampled in this study, would reduce our landscape-level estimate of C content in the top 15 m of yedoma from 205 kg C m^{-2} to 76-141 kg C m^{-2}, which is still an order of magnitude more C than is stored in the active layer and two orders of magnitude more C than is stored in biomass.

4.3 Micro-scale variation in soil carbon and thaw depth

In addition to the effects of parent material and climate on soil C storage, soil carbon pools are determined by the balance between biological inputs and losses due to microbial decomposition and lateral transport. These biological processes are, in turn, also heavily influenced by climate on regional and local scales. We found that soil samples with higher moisture content also had higher C density, which is likely due to both the effects of soil moisture on microbial activity and indirect effects of soil moisture on C inputs to soils through effects on plant productivity. In wetter soils, oxygen diffusion is limited, resulting in anaerobic conditions where microbial decomposition is slower, and C can accumulate at a higher rate than

437 in more well-drained, well-aerated soils (Schädel et al., 2016). However, this positive
438 association between moisture and C density may also be a result of increased C inputs and plant
439 productivity associated with higher soil moisture (Berner et al. 2013) or the lateral movement of
440 dissolved organic C into the wetter sites. It is likely that environmental controls on both C inputs
441 and losses are driving the patterns of C accumulation across the watershed.
442 Plant species composition may also play an important role in soil C storage in boreal
443 forests (Hollingsworth et al., 2008) through the quality and quantity of litter inputs and through
444 vegetation effects on environmental controls such as soil moisture and temperature. Lichens and
445 mosses are sometimes thought to encourage soil C storage through their promotion of low soil
446 temperatures, higher moisture, and a relatively acidic environment (Bonan and Shugar, 1989).
447 However, at our sites, increasing abundance of lichen and moss was associated with lower soil C
448 storage, which may have been due to lower rates of C fixation (Turetsky et al., 2010), higher
449 rates of decomposition of vascular plant litter in moss and lichen patches (Wardle et al., 2003),
450 or impacts of vegetation functional types on soil moisture and soil temperatures. Because the
451 interactions between soil processes and vegetation are bidirectional, the processes driving these
452 observed patterns are unclear and further experimental work is needed to identify the
453 mechanisms.
454 Increasing thaw depth may result in increased C loss from boreal ecosystems; as more
455 soil is thawed, more organic matter is available for decomposition. We found that thaw depth
456 was negatively related to stand age; the deeper thaw depth observed in the younger sites could be
457 a result of more recent burning events, which tend to increase thaw depth (O'Donnell et al.,
458 2011; Yoshikawa et al., 2002).
459

5 CONCLUSIONS

We found that the overwhelming majority of C in the Y4 watershed was stored belowground, but that the amount of C within any given pool was highly variable throughout the landscape; C storage in AGB varied up to 95% among sites, and there was 69% variation in the top 10 cm of soil, 36% in the top 30 cm, and 28% in the top 1 m. This variability among sites in our study was similar to the variability between our sites and others that were 3 to 50 km away (Matsuura et al., 2005; Palmtag et al., 2015), indicating a high level of natural variability at the meter and kilometer scales. Our results also indicate higher soil C variability in surface soils when compared to deeper soils, indicating that recent, on-going processes significantly contribute to soil C variability. Specifically, our results show that soil moisture, aboveground biomass, and vegetation community structure are influential in explaining near-surface belowground C storage. These linkages between above and belowground processes, such as the negative relationship between stand age and thaw depth, have important implications for soil C vulnerability as tree lines shift and biomass and stand structure are increasingly impacted by fire, climate, and direct human disturbances.

DATA AVAILABILITY

All data are available as supplemental material and through the Arctic Data Center through the following citation: Kathryn Heard, Susan Natali, Andrew Bunn, and Heather D. Alexander. 2015. Northeast Siberia Plant and Soil Data: Plant Composition and Cover, Plant and Soil Carbon Pools, and Thaw Depth. NSF Arctic Data Center. doi:10.5065/D6NG4NP0.

AUTHOR CONTRIBUTION

E. Webb contributed to data collection and processing and analyzed data, created figures, and drafted manuscript. K. Heard collected, processed, and summarized data and contributed to writing. S. Natali oversaw and contributed to data collection, processing, analysis, and writing. A. Bunn oversaw data collection, processing, and analysis. H. Alexander contributed to data collection, analysis, and writing. L. Berner contributed to data collection and processing and figure creation. M. Loranty contributed to data collection and processing. J. Schade contributed to lab analyses. V. Spektor and A. Kholodov collected and processed deep permafrost cores. N. Zimov contributed to data collection. All authors reviewed the manuscript and provided critical feedback.

COMPETING INTERESTS

The authors declare that they have no conflict of interest.

ACKNOWLEDGMENTS

This project was supported by funding from the National Geographic Society (Natali) and the National Science Foundation (NSF-1044610, NSF-1417745 NSF-1014180, NSF-1044417, NSF-1417700, NSF-1417908; Natali, Natali, Schade, Bunn, Loranty, Kholodov). We thank S. Shin and other Polaris Project 2013 participants for field and lab assistance, and the staff and scientists at the Northeast Science Station for logistical and field support.

REFERENCES

Alexander, H. D., Mack, M. C., Goetz, S., Loranty, M. M., Beck, P. S. A., Earl, K., Zimov, S., Davydov, S. and Thompson, C. C.: Carbon Accumulation Patterns During Post-Fire Succession in Cajander Larch (*Larix cajanderi*) Forests of Siberia, Ecosystems, 15(7), 1065–1082, doi:10.1007/s10021-012-9567-6, 2012.

508 Alexeyev, V. A. and Birdsey, R. A.: Carbon Storage in Forests and Peatlands of Russia, Radnor,
509 PA., 1998.
510 Beck, P. S. A., Juday, G. P., Alix, C., Barber, V. A., Winslow, S. E., Sousa, E. E., Heiser, P.,
511 Herriges, J. D. and Goetz, S. J.: Changes in forest productivity across Alaska consistent
512 with biome shift, Ecol. Lett., 14, 373–379, doi:10.1111/j.1461-0248.2011.01598.x, 2011.
513 Beer, C.: Permafrost Sub-grid Heterogeneity of Soil Properties Key for 3-D Soil Processes and
514 Future Climate Projections, Front. Earth Sci., 4(August), 1–7,
515 doi:10.3389/feart.2016.00081, 2016.
516 Berg, E. E., Henry, J. D., Fastie, C. L., Volder, A. D. De and Matsuoka, S. M.: Spruce beetle
517 outbreaks on the Kenai Peninsula , Alaska , and Kluane National Park and Reserve ,
518 Yukon Territory : Relationship to summer temperatures and regional differences in
519 disturbance regimes, For. Ecol. Manage., 227, 219–232,
520 doi:10.1016/j.foreco.2006.02.038, 2006.
521 Berner, L. T., Beck, P. S. A., Loranty, M. M., Alexander, H. D., MacK, M. C. and Goetz, S. J.:
522 Cajander larch (Larix cajanderi) biomass distribution, fire regime and post-fire recovery
523 in northeastern Siberia, Biogeosciences, 9(10), 3943–3959, doi:10.5194/bg-9-3943-2012,
524 2012.
525 Berner, L. T., Beck, P. S. A., Bunn, A. G. and Goetz, S. J.: Plant response to climate change
526 along the forest-tundra ecotone in northeastern Siberia, Glob. Chang. Biol., 19(11),
527 3449–3462, doi:10.1111/gcb.12304, 2013.
528 Berner, L. T., Alexander, H. D., Loranty, M. M., Ganzlin, P., Mack, M. C., Davydov, S. P. and
529 Goetz, S. J.: Biomass allometry for alder, dwarf birch, and willow in boreal forest and
530 tundra ecosystems of far northeastern Siberia and north-central Alaska, For. Ecol.
531 Manage., 337, 110–118, doi:10.1016/j.foreco.2014.10.027, 2015.
532 Bonan, G. B. . and Shugar, H. H. .: Environmental Factors and Ecological Processes in Boreal
533 Forests, Annu. Rev. Ecol. Syst., 20, 1–28, 1989.
534 Bradshaw, C. and Warkentin, I. G.: Global estimates of boreal forest carbon stocks and flux,
535 Glob. Planet. Change, 128(February), 24–30, doi:10.1016/j.gloplacha.2015.02.004, 2015.
536 Brown, J. K.: Handbook for Inventorying Downed Woody Material, Ogden, Utah., 1974.
537 Burnham, K. P. and Anderson, D. R.: Model Selection and Multimodel Inference: A Practical
538 Information-Theoretic Approach, 2nd ed., Springer, New York., 2002.
539 Carvalhais, N., Forkel, M., Khomik, M., Bellarby, J., Jung, M., Migliavacca, M., Mu, M.,
540 Saatchi, S., Santoro, M., Thurner, M., Weber, U., Ahrens, B., Beer, C., Cescatti, A.,
541 Randerson, J. T., Reichstein, M., Mu, M., Saatchi, S., Santoro, M., Thurner, M., Weber,
542 U., Ahrens, B., Beer, C., Cescatti, A., Randerson, J. T., Reichstein, M., Mu, M., Saatchi,
543 S., Santoro, M., Thurner, M., Weber, U., Ahrens, B., Beer, C., Cescatti, A., Randerson, J.
544 T. and Reichstein, M.: Global covariation of carbon turnover times with climate in
545 terrestrial ecosystems, Nature, 514(7521), 213–217, doi:10.1038/nature13731, 2014.
546 Chapin, F. S., McGuire, A. D., Randerson, J., Pielske, R., Baldocchi, D., Hobbie, S. E., Roulet,
547 N., Eugster, W., Kasischke, E. S., Rastetter, E. B., Zimov, S. A. and Running, S. W.:
548 Arctic and boreal ecosystmes of western North America as components of the climate
549 system, Glob. Chang. Biol., 6, 211–223, 2000.
550 Chapin, F. S., Euskirchen, E. S., Tape, K. D., Thompson, C. D. C., Walker, D. A., McGuire, A.
551 D., Rupp, T. S., Hinzman, L. D., Sturm, M., Serreze, M. C., McFadden, J. P., Key, J. R.,
552 Lloyd, A. H., Lynch, A. H., Beringer, J., Schimel, J. P., Chapman, W. L., Epstein, H. E.,
553 Jia, G., Ping, C.-L. L., Welker, J. M., McGuire, A. D., Rupp, T. S., Lynch, A. H.,

554 Schimel, J. P., Beringer, J., Chapman, W. L., Epstein, H. E., Euskirchen, E. S., Hinzman,
555 L. D., Jia, G., Ping, C.-L. L., Tape, K. D., Thompson, C. D. C., Walker, D. A. and
556 Welker, J. M.: Role of land-surface changes in arctic summer warming, Science (80-.).,
557 310(5748), 657, doi:10.1126/science.1117368, 2005.
558 Chen, J. M., Rich, P. M., Gower, S. T., Norman, J. M. and Plummer, S.: Leaf area index of
559 boreal forests: Theory, techniques, and measurements, J. Geophys. Res., 102(D24), 429–
560 443, doi:10.1029/97JD01107, 1997.
561 Chen, J. M., Menges, C. H. and Leblanc, S. G.: Global mapping of foliage clumping index using
562 multi-angular satellite data, Remote Sens. Environ., 97(4), 447–457,
563 doi:10.1016/j.rse.2005.05.003, 2005.
564 Christensen, J. H., Kumar, K. K., Aldrian, E., An, S.-I., Cavalcanti, I. F. A., Castro, M. de, Dong,
565 W., Goswami, P., Hall, A., Kanyanga, J. K., Kitoh, A., Kossin, J., Lau, N.-C., Renwick,
566 J., Stephenson, D. B., Xie, S.-P. and Zhou, T.: Climate Phenomena and their Relevance
567 for Future Regional Climate Change., in Climate Change 2013: The Physical Science
568 Basis. Contribution of Working Group 1 to the fifth Assessment Report of the
569 Intergovernmental Panel on Climate Change, edited by T. . Stocker, D. Qin, G.-K.
570 Plattner, M. Tignor, S. K. Allen, J. Boschung, A. Nauels, Y. Xia, V. Bex, and P. M.
571 Midgley, Cambridge University Press, Cambridge, United Kingdom and New York, NY,
572 USA., 2013.
573 Elmendorf, S. C., Henry, G. H. R., Hollister, R. D., Björk, R. G., Boulanger-Lapointe, N.,
574 Cooper, E. J., Cornelissen, J. H. C., Day, T. A., Dorrepaal, E., Elumeeva, T. G., Gill, M.,
575 Gould, W. A., Harte, J., Hik, D. S., Hofgaard, A., Johnson, D. R., Johnstone, J. F.,
576 Jónsdóttir, I. S., Jorgenson, J. C., Klanderud, K., Klein, J. A., Koh, S., Kudo, G., Lara,
577 M., Lévesque, E., Magnússon, B., May, J. L., Mercado-Dı´az, J. A., Michelsen, A.,
578 Molau, U., Myers-Smith, I. H., Oberbauer, S. F., Onipchenko, V. G., Rixen, C., Schmidt,
579 N. M., Shaver, G. R., Spasojevic, M. J., Þórhallsdóttir, Þ. E., Tolvanen, A., Troxler, T.,
580 Tweedie, C. E., Villareal, S., Wahren, C.-H., Walker, X., Webber, P. J., Welker, J. M.
581 and Wipf, S.: Plot-scale evidence of tundra vegetation change and links to recent summer
582 warming, Nat. Clim. Chang., 2(6), 453–457, doi:10.1038/nclimate1465, 2012.
583 Euskirchen, E. S., Mcguire, a D., Chapin, F. S., Yi, S., Thompson, C. C. and Thompson3, C. C.:
584 Changes in Vegetation in Northern Alaska under Scenarios of Climate Change, 2003–
585 2100: Implications for Climate Feedbacks Changes in vegetation in northern Alaska
586 under scenarios of climate change, 2003-2100: implications for climate feedbacks, Ecol.
587 Appl., 19(194), 1022–1043, doi:10.1890/08-0806.1, 2009.
588 Fisher, J. P., Estop-Aragones, C., Thierry, A., Charman, D. J., Wolfe, S. A., Hartley, I. P.,
589 Murton, J. B., Williams, M. and Phoenix, G. K.: The influence of vegetation and soil
590 characteristics on active-layer thickness of permafrost soils in boreal forest, Glob. Chang.
591 Biol., 22(9), 3127–3140, doi:10.1111/gcb.13248, 2016.
592 Fu, P. and Rich, P.: A geometric solar radiation model with applications in agriculture and
593 forestry, Comput. Electron. Agric., 37(1–3), 25–35, doi:10.1016/S0168-1699(02)00115-
594 1, 2002.
595 Goetz, S. J., Mack, M. C., Gurney, K. R., Randerson, J. T. and Houghton, R. A.: Ecosystem
596 responses to recent climate change and fire disturbance at northern high latitudes:
597 observations and model results contrasting northern Eurasia and North America, Environ.
598 Res. Lett., 2(4), 45031, doi:10.1088/1748-9326/2/4/045031, 2007.
599 Grosse, G., Robinson, J., Bryant, R., Taylor, M. D., Harper, W., DeMasi, A., Kyker-Snowman,

E. Veremeeva, A., Schirrmeister, L. and Harden, J.: Distribution of late Pleistocene ice-rich syngenetic permafrost of the Yedoma Suite in east and central Siberia, Russia, Geol. Surv. Open File Rep. 2013-1078, 37pp [online] Available from: http://epic.awi.de/33878/, 2013.

Guay, K. C., Beck, P. S. A., Berner, L. T., Goetz, S. J., Baccini, A. and Buermann, W.: Vegetation productivity patterns at high northern latitudes: A multi-sensor satellite data assessment, Glob. Chang. Biol., 20(10), 3147–3158, doi:10.1111/gcb.12647, 2014.

Harden, J. W., Koven, C. D., Ping, C.-L., Hugelius, G., David McGuire, a., Camill, P., Jorgenson, T., Kuhry, P., Michaelson, G. J., O'Donnell, J. a., Schuur, E. a. G., Tarnocai, C., Johnson, K. and Grosse, G.: Field information links permafrost carbon to physical vulnerabilities of thawing, Geophys. Res. Lett., 39(15), 1–6, doi:10.1029/2012GL051958, 2012.

Hobbie, S. E., Schimel, J. P., Trumbore, S. E. and Randerson, J. R.: Controls over carbon storage and turnover in high-latitude soils, Glob. Chang. Biol., 6(S1), 196–210, doi:10.1046/j.1365-2486.2000.06021.x, 2000.

Hollingsworth, T. N., Schuur, E. A. G., Chapin, F. S. and Walker, M. D.: Plant community composition as a predictor of regional soil carbon storage in Alaskan boreal black spruce ecosystems, Ecosystems, 11(4), 629–642, doi:10.1007/s10021-008-9147-y, 2008.

Holmes, R. M., McClelland, J. W., Peterson, B. J., Tank, S. E., Bulygina, E., Eglinton, T. I., Gordeev, V. V., Gurtovaya, T. Y., Raymond, P. A., Repeta, D. J., Staples, R., Striegl, R. G., Zhulidov, A. V. and Zimov, S. A.: Seasonal and Annual Fluxes of Nutrients and Organic Matter from Large Rivers to the Arctic Ocean and Surrounding Seas, Estuaries and Coasts, 35(2), 369–382, doi:10.1007/s12237-011-9386-6, 2012.

Hugelius, G., Strauss, J., Zubrzycki, S., Harden, J. W., Schuur, E. A. G., Ping, C. L., Schirrmeister, L., Grosse, G., Michaelson, G. J., Koven, C. D., O'Donnell, J. A., Elberling, B., Mishra, U., Camill, P., Yu, Z., Palmtag, J. and Kuhry, P.: Estimated stocks of circumpolar permafrost carbon with quantified uncertainty ranges and identified data gaps, Biogeosciences, 11(23), 6573–6593, doi:10.5194/bg-11-6573-2014, 2014.

Jean, M. and Payette, S.: Effect of vegetation cover on the ground thermal regime of wooded and non-wooded palsas, Permafr. Periglac. Process., 25(4), 281–294, doi:10.1002/ppp.1817, 2014.

Johnson, K. D., Harden, J., McGuire, A. D., Bliss, N. B., Bockheim, J. G., Clark, M., Nettleton-Hollingsworth, T., Jorgenson, M. T., Kane, E. S., Mack, M., O'Donnell, J., Ping, C. L., Schuur, E. A. G., Turetsky, M. R. and Valentine, D. W.: Soil carbon distribution in Alaska in relation to soil-forming factors, Geoderma, 167–168, 71–84, doi:10.1016/j.geoderma.2011.10.006, 2011.

Kajimoto, T., Matsuura, Y., Osawa, A., Abaimov, A. P., Zyryanova, O. A., Isaev, A. P. and Yefremov, D. P.: Size – mass allometry and biomass allocation of two larch species growing on the continuous permafrost region in Siberia, For. Ecol. Manage., 222, 314–325, doi:10.1016/j.foreco.2005.10.031, 2006.

Kajimoto, T., Osawa, A., Usoltsev, V. A. and Abaimov, A. P.: Biomass and Productivity of Siberian Larch Forest Ecosystems, in Permafrost Ecosystems: Siberian Larch Forests, vol. 209, edited by A. Osawa, O. Zyryanova, Y. Matsuura, T. Kajimoto, and R. Wein, pp. 99–120, Springer., 2010.

Kasischke, E. S. and Turetsky, M. R.: Recent changes in the fire regime across the North American boreal region - Spatial and temporal patterns of burning across Canada and

Alaska, Geophys. Res. Lett., 33(9), 1–5, doi:10.1029/2006GL025677, 2006.
Koven, C. D., Schuur, E. A. G., Schädel, C., Bohn, T. J., Burke, E. J., Chen, G., Chen, X., Ciais, P., Grosse, G., Harden, J. W., Hayes, D. J., Hugelius, G., Jafarov, E. E., Krinner, G., Kuhry, P., Lawrence, D. M., MacDougall, A. H., Marchenko, S. S., McGuire, A. D., Natali, S. M., Nicolsky, D. J., Olefeldt, D., Peng, S., Romanovsky, V. E., Schaefer, K. M., Strauss, J., Treat, C. C. and Turetsky, M.: A simplified, data-constrained approach to estimate the permafrost carbon–climate feedback, Philos. Trans. R. Soc. A Math. Phys. Eng. Sci., 373(2054), 20140423, doi:10.1098/rsta.2014.0423, 2015.
Kurz, W. A., Dymond, C. C., Stinson, G., Rampley, G. J., Neilson, E. T., Carroll, A. L., Ebata, T. and Safranyik, L.: Mountain pine beetle and forest carbon feedback to climate change., Nature, 452(7190), 987–90, doi:10.1038/nature06777, 2008.
Liljedahl, A. K., Boike, J., Daanen, R. P., Fedorov, A. N., Frost, G. V., Grosse, G., Hinzman, L. D., Iijma, Y., Jorgenson, J. C., Matveyeva, N., Necsoiu, M., Raynolds, M. K., Romanovsky, V. E., Schulla, J., Tape, K. D., Walker, D. A., Wilson, C., Yabuki, H. and Zona, D.: Pan-Arctic ice-wedge degradation in warming permafrost and influence on tundra hydrology, Nat. Geosci., 9(April), 312–318, doi:10.1038/ngeo2674, 2016.
Lloyd, A. H.: Ecological Histories from Alaskan Tree Lines Provide Insight into Future Change. Author(s): Andrea H . Lloyd Published by : Wiley Stable URL : http://www.jstor.org/stable/3450611 Linked references are available on JSTOR for this article : You, Ecology, 86(7), 1687–1695, 2005.
Loranty, M. M., Berner, L. T., Goetz, S. J., Jin, Y. and Randerson, J. T.: Vegetation controls on northern high latitude snow-albedo feedback: Observations and CMIP5 model simulations, Glob. Chang. Biol., 20(2), 594–606, doi:10.1111/gcb.12391, 2014.
Loranty, M. M., Lieberman-Cribbin, W., Berner, L. T., Natali, S. M., Goetz, S. J., Alexander, H. D. and Kholodov, A. L.: Spatial variation in vegetation productivity trends, fire disturbance, and soil carbon across arctic-boreal permafrost ecosystems, Environ. Res. Lett., 11(9), 95008, doi:10.1088/1748-9326/11/9/095008, 2016.
Mack, M. C., Schuur, E. a G., Bret-Harte, M. S., Shaver, G. R. and Chapin, F. S.: Ecosystem carbon storage in arctic tundra reduced by long-term nutrient fertilization., Nature, 431(7007), 440–3, doi:10.1038/nature02887, 2004.
Matsuura, Y. and Hirobe, M.: Soil Carbon and Nitrogen , and Characteristics of Soil Active Layer in Siberian Permafrost Region, in Permafrost Ecosystems: Siberian Larch Forests, vol. 209, edited by A. Osawa, O. Zyryanova, Y. Matsuura, T. Kajimoto, and R. Wein, pp. 149–163, Springer., 2010.
Matsuura, Y., Kajimoto, T., Osawa, A. and Abaimov, A. P.: Carbon storage in larch ecosystems in continuous permafrost region of Siberia, Phyt. - Ann. Rei Bot., 45(4), 51–54, 2005.
Mishra, U. and Riley, W. J.: Alaskan soil carbon stocks: Spatial variability and dependence on environmental factors, Biogeosciences, 9(9), 3637–3645, doi:10.5194/bg-9-3637-2012, 2012.
Mishra, U., Jastrow, J. D., Matamala, R., Hugelius, G., Koven, C. D., Harden, J. W., Ping, C. L., Michaelson, G. J., Fan, Z., Miller, R. M., McGuire, a D., Tarnocai, C., Kuhry, P., Riley, W. J., Schaefer, K., Schuur, E. a G., Jorgenson, M. T. and Hinzman, L. D.: Empirical estimates to reduce modeling uncertainties of soil organic carbon in permafrost regions: a review of recent progress and remaining challenges, Environ. Res. Lett., 8(3), 35020, doi:10.1088/1748-9326/8/3/035020, 2013.
Myers-Smith, I. H., Elmendorf, S. C., Beck, P. S. a, Wilmking, M., Hallinger, M., Blok, D.,

692 Tape, K. D., Rayback, S. a, Macias-Fauria, M., Forbes, B. C., Speed, J. D. M.,
693 Boulanger-Lapointe, N., Rixen, C., Levesque, E., Schmidt, N. M., Baittinger, C., Trant,
694 A. J., Hermanutz, L., Collier, L. S., Dawes, M. a, Lantz, T. C., Weijers, S., Jorgensen, R.
695 H., Buchwal, A., Buras, A., Naito, A. T., Ravolainen, V., Schaepman-Strub, G., Wheeler,
696 J. a, Wipf, S., Guay, K. C., Hik, D. S. and Vellend, M.: Climate sensitivity of shrub
697 growth across the tundra biome, Nat. Clim. Chang., advance on(September), 1–44,
698 doi:10.1038/nclimate2697, 2015.
699 Nalder, I. a, Wein, R. W., Alexander, M. E. and de Groot, W. J.: Physical properties of dead and
700 downed round-wood fuels in the boreal forests of Alberta and Northwest Territories, Int.
701 J. Wildl. Fire, 27(9), 1513–1517, doi:10.1139/x97-083, 1997.
702 O'Donnell, J. A., Harden, J. W., Mcguire, A. D., Kanevskiy, M. Z., Jorgenson, M. T. and Xu, X.:
703 The effect of fire and permafrost interactions on soil carbon accumulation in an upland
704 black spruce ecosystem of interior Alaska: Implications for post-thaw carbon loss, Glob.
705 Chang. Biol., 17(3), 1461–1474, doi:10.1111/j.1365-2486.2010.02358.x, 2011.
706 Osawa, A. and Kajimoto, T.: Development of Stand Structure in Larch Forests, in Permafrost
707 Ecosystems: Siberian Larch Forests, vol. 209, edited by A. Osawa, O. Zyryanova, Y.
708 Matsuura, T. Kajimoto, and R. Wein, pp. 123–148, Springer., 2010.
709 Palmtag, J., Hugelius, G., Lashchinskiy, N., Tamstorf, M. P., Richter, A., Elberling, B. and
710 Kuhry, P.: Storage, landscape distribution, and burial history of soil organic matter in
711 contrasting areas of continuous permafrost, Arctic, Antarct. Alp. Res., 47(1), 71–88,
712 doi:10.1657/aaar0014-027, 2015.
713 Pan, Y., Birdsey, R. a, Fang, J., Houghton, R., Kauppi, P. E., Kurz, W. a, Phillips, O. L.,
714 Shvidenko, A., Lewis, S. L., Canadell, J. G., Ciais, P., Jackson, R. B., Pacala, S. W.,
715 McGuire, a D., Piao, S., Rautiainen, A., Sitch, S. and Hayes, D.: A large and persistent
716 carbon sink in the world's forests., Science, 333(6045), 988–93,
717 doi:10.1126/science.1201609, 2011.
718 Pearson, R. G., Phillips, S. J., Loranty, M. M., Beck, P. S. A., Damoulas, T., Knight, S. J. and
719 Goetz, S. J.: Shifts in Arctic vegetation and associated feedbacks under climate change,
720 Nat. Clim. Chang., 3(7), 673–677, doi:10.1038/nclimate1858, 2013.
721 Pinherio, J., Bates, D., Saikat, D. and Sarkar, D.: nlme: Linear and nonlinear mixed effects
722 models. R package, R-core, 2013.
723 R Core Development Team: R: A language and environment for statistical computing., [online]
724 Available from: http://www.r-project.org/, 2012.
725 Rich, P. M., Dubayah, R., Hetrick, W. A., Saving, S. C. and Dubayah, R. O.: Using Viewshed
726 Models to Calculate Intercepted Solar Radiation: Applications in Ecology, Am. Soc.
727 Photogramm. Remote Sens. Tech. Pap., 524–529, 1994.
728 Rogers, B. M., Soja, A. J., Goulden, M. L. and Randerson, J. T.: Influence of tree species on
729 continental differences in boreal fires and climate feedbacks, Nat. Geosci., 8(February),
730 228–234, doi:10.1016/j.cognition.2008.05.007, 2015.
731 Salmon, V. G., Soucy, P., Mauritz, M., Celis, G., Natali, S. M., Mack, M. C. and Schuur, E. A.
732 G.: Nitrogen availability increases in a tundra ecosystem during five years of
733 experimental permafrost thaw, Glob. Chang. Biol., 22(5), 1927–1941,
734 doi:10.1111/gcb.13204, 2016.
735 Schädel, C., Schuur, E. A. G., Bracho, R., Elberling, B., Knoblauch, C., Lee, H., Luo, Y.,
736 Shaver, G. R. and Turetsky, M. R.: Circumpolar assessment of permafrost C quality and
737 its vulnerability over time using long-term incubation data., Glob. Chang. Biol., 20(2),

641–52, doi:10.1111/gcb.12417, 2014.
Schädel, C., Bader, M. K.-F., Schuur, E. A. G., Biasi, C., Bracho, R., Čapek, P., De Baets, S., Diáková, K., Ernakovich, J., Estop-Aragones, C., Graham, D. E., Hartley, I. P., Iversen, C. M., Kane, E., Knoblauch, C., Lupascu, M., Martikainen, P. J., Natali, S. M., Norby, R. J., O'Donnell, J. A., Chowdhury, T. R., Šantrůčková, H., Shaver, G., Sloan, V. L., Treat, C. C., Turetsky, M. R., Waldrop, M. P. and Wickland, K. P.: Potential carbon emissions dominated by carbon dioxide from thawed permafrost soils, Nat. Clim. Chang., 6(June), 1–5, doi:10.1038/nclimate3054, 2016.
Schirrmeister, L., Grosse, G., Wetterich, S., Overduin, P. P., Strauss, J., Schuur, E. A. G. and Hubberten, H. W.: Fossil organic matter characteristics in permafrost deposits of the northeast Siberian Arctic, J. Geophys. Res. Biogeosciences, 116(3), doi:10.1029/2011JG001647, 2011.
Schneider Von Deimling, T., Grosse, G., Strauss, J., Schirrmeister, L., Morgenstern, A., Schaphoff, S., Meinshausen, M. and Boike, J.: Observation-based modelling of permafrost carbon fluxes with accounting for deep carbon deposits and thermokarst activity, Biogeosciences, 12(11), 3469–3488, doi:10.5194/bg-12-3469-2015, 2015.
Schuur, E. A. G., McGuire, A. D., Grosse, G., Harden, J. W., Hayes, D. J., Hugelius, G., Koven, C. D. and Kuhry, P.: Climate change and the permafrost carbon feedback, Nature, 520(January 2016), 171–179, doi:10.1038/nature14338, 2015.
Shmelev, D., Veremeeva, A., Kraev, G., Kholodov, A., Spencer, R. G. M. and Walker, W. S.: Estimation and Sensitivity of Carbon Storage in Permafrost of North-Eastern Yakutia, Permafr. Periglac. Process., (August 2016), doi:10.1002/ppp.1933, 2017.
Shuman, J. K., Shugart, H. H. and Krankina, O. N.: Assessment of carbon stores in tree biomass for two management scenarios in Russia, Environ. Res. Lett., 8(4), 1–9, doi:10.1088/1748-9326/8/4/045019, 2013.
Siewert, M. B., Hanisch, J., Weiss, N., Kuhry, P., Maximov, T.C. and Hugelius G. (2015), Comparing carbon storage of Siberian tundra and taiga permafrost ecosystems at very high spatial resolution, J. Geophys. Res. Biogeosci., 120, 1973–1994, doi:10.1002/2015JG002999.
Soja, A. J., Shugart, H. H., Sukhinin, A., Conard, S. and Stackhouse, P. W.: Satelliet-Derived Mean Fire Return Intervals As Indicators of Change in Siberia (1995 – 2002), Mitig. Adapt. Strateg. Glob. Chang., 75–96, 2006.
Soja, A. J., Tchebakova, N. M., French, N. H. F., Flannigan, M. D., Shugart, H. H., Stocks, B. J., Sukhinin, A. I., Parfenova, E. I., Chapin, F. S. and Stackhouse, P. W.: Climate-induced boreal forest change: Predictions versus current observations, Glob. Planet. Change, 56(3–4), 274–296, doi:10.1016/j.gloplacha.2006.07.028, 2007.
Stolbovoi, V.: Soil carbon in the forests of Russia, Mitig. Adapt. Strateg. Glob. Chang., 11(1), 203–222, doi:10.1007/s11027-006-1021-7, 2006.
Strauss, J., Schirrmeister, L., Grosse, G., Wetterich, S., Ulrich, M., Herzschuh, U. and Hubberten, H. W.: The deep permafrost carbon pool of the Yedoma region in Siberia and Alaska, Geophys. Res. Lett., 40(23), 6165–6170, doi:10.1002/2013GL058088, 2013.
Sturm, M., Schimel, J., Michaelson, G., Welker, J. M., Oberbauer, S. F., Liston, G. E., Fahnestock, J. and Romanovsky, V. E.: Winter Biological Processes Could Help Convert Arctic Tundra to Shrubland, Bioscience, 55(1), 17, doi:10.1641/0006-3568(2005)055[0017:WBPCHC]2.0.CO;2, 2005.
Swann, A. L., Fung, I. Y., Levis, S., Bonan, G. B. and Doney, S. C.: Changes in Arctic

784 vegetation amplify high-latitude warming through the greenhouse effect, Proc. Natl.
785 Acad. Sci., 107(4), 1295–1300, doi:10.1073/pnas.0913846107, 2010.
786 Tarnocai, C., Canadell, J. G., Schuur, E. a. G., Kuhry, P., Mazhitova, G. and Zimov, S.: Soil
787 organic carbon pools in the northern circumpolar permafrost region, Global Biogeochem.
788 Cycles, 23(2), doi:10.1029/2008GB003327, 2009.
789 Tautenhahn, S., Lichstein, J. W., Jung, M., Kattge, J., Bohlman, S. A., Heilmeier, H.,
790 Prokushkin, A., Kahl, A. and Wirth, C.: Dispersal limitation drives successional
791 pathways in Central Siberian forests under current and intensified fire regimes, Glob.
792 Chang. Biol., 22(6), 2178–2197, doi:10.1111/gcb.13181, 2016.
793 Ter-Mikaelian, M. T., Colombo, S. J. and Chen, J.: Amount of downed woody debris and its
794 prediction using stand characteristics in boreal and mixedwood forests of Ontario,
795 Canada, Can. J. For. Res., 38(8), 2189–2197, doi:10.1139/X08-067, 2008.
796 Trahan, M. W. and Schubert, B. A.: Temperature-induced water stress in high-latitude forests in
797 response to natural and anthropogenic warming, Glob. Chang. Biol., 22(2), 782–791,
798 doi:10.1111/gcb.13121, 2016.
799 Trumbore, S. E. and Harden, J. W.: Accumulation and turnover of carbon in organic and mineral
800 soils of the BOREAS northern study area, J. Geophys. Res., 102(D24), 817–28, 1997.
801 Turetsky, M. R., Mack, M. C., Hollingsworth, T. N. and Harden, J. W.: The role of mosses in
802 ecosystem succession and function in Alaska's boreal forest, Can. J. For. Res., 40(7),
803 1288–1301, doi:10.1139/X10-081, 2010.
804 Ulrich, M., Grosse, G., Strauss, J. and Schirrmeister, L.: Quantifying Wedge-Ice Volumes in
805 Yedoma and Thermokarst Basin Deposits, Permafr. Periglac. Process., 25, 151–161,
806 doi:10.1002/ppp.1810, 2014.
807 Vitharana, U. W. A., Mishra, U., Jastrow, J. D., Matamala, R. and Fan, Z.: Observational needs
808 for estimating Alaskan soil carbon stocks under current and future climate, J. Geophys.
809 Res. Biogeosci., 122, 415–429, doi:10.1002/2016JG003421, 2017..
810 Walker, X. J., Mack, M. C. and Johnstone, J. F.: Stable carbon isotope analysis reveals
811 widespread drought stress in boreal black spruce forests, Glob. Chang. Biol., 21(8),
812 3102–3113, doi:10.1111/gcb.12893, 2015.
813 Walter Anthony, K. M., Zimov, S. a., Grosse, G., Jones, M. C., Anthony, P. M., Iii, F. S. C.,
814 Finlay, J. C., Mack, M. C., Davydov, S., Frenzel, P. and Frolking, S.: A shift of
815 thermokarst lakes from carbon sources to sinks during the Holocene epoch, Nature,
816 511(7510), 452–456, doi:10.1038/nature13560, 2014.
817 Wardle, D. A., Nilsson, M. C., Zackrisson, O. and Gallet, C.: Determinants of litter mixing
818 effects in a Swedish boreal forest, Soil Biol. Biochem., 35(6), 827–835,
819 doi:10.1016/S0038-0717(03)00118-4, 2003.
820 Yoshikawa, K., Bolton, W. R., Romanovsky, V. E., Fukuda, M. and Hinzman, L. D.: Impacts of
821 wildfire on the permafrost in the boreal forests of Interior Alaska, J. Geophys. Res.,
822 108(D1), 16–17, doi:10.1029/2001JD000438, 2002.
823 Zimov, S. A., Davydov, S. P., Zimova, G. M., Davydova, A. I., Schuur, E. A. G., Dutta, K. and
824 Chapin, I. S.: Permafrost carbon: Stock and decomposability of a globally significant
825 carbon pool, Geophys. Res. Lett., 33(20), 1–5, doi:10.1029/2006GL027484, 2006.
826 Zuur, A. F., Ieno, E. N., Walker, N. J., Saveliev, A. A. and Smith, G. M.: Mixed Effects Models
827 and Extensions in Ecology with R., 2009.
828
829

FIGURE DESCRIPTIONS

Figure 1. Location of the Y4 watershed in relation to Russia (inset) and location of the sampling sites within the Y4 catchment.

Figure 2. Average carbon density of all sites in the Y4 watershed (top: above and belowground to 1 m; bottom: aboveground only). Bars indicate standard error.

Figure 3. Relationship between thaw depth and stand age. Each point represents the average thaw depth measurement taken along a transect (three transects/site) and the stand age of the entire site. Thaw depths were measured in July/August of 2012 and 2013.

Figure 4. Relationship between SOC in the top 10 cm of soil and moisture, moss cover, and lichen cover. Each point represents the average SOC measured at each transect (three transects/site) and its corresponding moisture content or the average moss or lichen cover measured at that transect.

Figure 5. Bulk density, carbon density, and ice content of the two deep (15 m) permafrost soil cores.

849 **TABLES**

Table 1: Site Characteristics. All sites were in forested areas except #17 (riparian); Site #18 (alas) had few scattered trees located along one end of the sampling transects.

Site Number	Latitude (Degrees North)	Longitude (Degrees East)	Slope (Degrees)	Aspect (Degrees)	Summer Insolation (WH m^{-2})	Stand Age (yrs)
1	68.74747	161.38988	5	160	4507	155
2	68.74529	161.38908	10	8	3950	167
3	68.74472	161.41486	14	249	4399	203
4	68.74164	161.41562	9	245	4409	23
5	68.74834	161.41350	10	357	3954	218
6	68.74939	161.41759	8	225	4509	205
7	68.74915	161.39000	5	57	4239	155
8	68.74932	161.38820	7	36	4132	208
9	68.75267	161.38544	8	340	4038	202
10	68.75352	161.39455	16	72	4008	211
11	68.74869	161.40834	10	222	4533	123
12	68.74837	161.40237	10	63	4121	71
13	68.74660	161.40433	17	61	3856	179
14	68.74513	161.40063	1	103	4361	40
15	68.75188	161.39095	3	237	4410	221
16	68.75519	161.40013	3	294	4307	200
17	68.74152	161.41411	8	225	4479	-
18	68.74632	161.38776	3	84	4314	-
19	68.74479	161.38410	6	61	4231	26
20	68.74333	161.40688	5	124	4429	-

850

Table 2: Leaf area index (LAI), tree and snag density, and percent cover of the 20 plots in the Y4 watershed. Values in parenthesis are standard error of the mean. Other cover includes woody debris and bare ground.

Site Number	LAI (Hemispherical Photography)	LAI (LAI-2000)	Larch Density (trees/m^2)	Snag Density (snags/m^2)	Canopy Cover (%)	Understory Shrub Cover (%)	Herbaceous cover (%)	Moss Cover (%)	Lichen Cover (%)	Other Cover (%)
1	0.03 (0.00)	0.13	0.09 (0.05)	0.00	22.4 (3.2)	45.2 (2.7)	3.5 (1.7)	22.0 (3.4)	15.6 (4.9)	12.4 (3.4)
2	0.22 (0.02)	0.13	0.04 (0.00)	0.00	16.0 (4.0)	49.4 (5.4)	4.8 (2.4)	25.0 (4.4)	6.9 (2.9)	13.8 (6.0)
3	0.53 (0.03)	0.68	0.08 (0.03)	0.00	43.2 (7.4)	60.3 (9.0)	0.7 (0.3)	31.3 (9.4)	3.4 (2.6)	4.3 (0.6)
4	0.02 (0.01)	0.00	0.08 (0.07)	0.00	2.6 (2.6)	72.3 (7.9)	2.5 (1.6)	7.4 (2.4)	3.4 (2.1)	14.3 (5.7)
5	0.37 (0.05)	1.35	0.08 (0.02)	0.03 (0.01)	32.3 (7.6)	51.5 (4.9)	4.2 (1.4)	14.4 (2.9)	16.9 (4.1)	13.1 (2.4)
6	0.38 (0.03)	0.47	0.06 (0.01)	0.03 (0.01)	26.0 (4.6)	57.9 (7.2)	8.4 (5.9)	17.4 (5.2)	3.6 (1.3)	12.1 (3.8)
7	0.15 (0.08)	0.00	0.05 (0.02)	0.00	17.6 (8.4)	34.8 (3.5)	3.4 (0.8)	34.0 (7.1)	22.8 (6.4)	4.8 (1.9)
8	0.06 (0.04)	0.29	0.02 (0.00)	0.00	7.0 (2.1)	34.8 (4.5)	3.8 (1.8)	32.5 (7.9)	24.8 (9.5)	4.0 (2.3)
9	0.07 (0.02)	0.00	0.01 (0.00)	0.00	9.4 (1.6)	44.2 (5.5)	0.0	33.5 (5.0)	16.7 (7.6)	5.6 (1.6)
10	0.30 (0.09)	1.41	0.08 (0.04)	0.04 (0.02)	24.3 (6.2)	49.2 (10.6)	8.6 (2.9)	29.8 (8.8)	5.3 (1.4)	7.1 (2.5)
11	0.05 (0.03)	0.22	0.02 (0.01)	0.00	4.7 (1.5)	33.6 (6.9)	5.8 (3.0)	15.3 (4.5)	30.6 (8.0)	15.0 (5.9)
12	0.01 (0.00)	0.00	0.02 (0.01)	0.00	0.0 (0.0)	47.1 (7.4)	7.5 (4.0)	20.2 (3.7)	19.0 (5.3)	6.9 (3.2)
13	0.23 (0.07)	0.82	0.07 (0.01)	0.02 (0.01)	18.9 (3.0)	47.4 (8.1)	4.2 (2.6)	25.6 (8.2)	13.6 (6.2)	9.1 (0.8)
14	0.00 (0.00)	0.00	0.03 (0.02)	0.00	0.8 (0.8)	47.2 (12.0)	5.8 (3.7)	11.3 (3.8)	33.5 (13.9)	2.3 (1.1)
15	0.03 (0.01)	0.00	0.02 (0.01)	0.00	3.8 (1.0)	41.3 (3.9)	3.8 (1.7)	22.4 (4.5)	21.9 (4.6)	10.4 (5.5)
16	0.31 (0.13)	0.88	0.05 (0.01)	0.00	18.5 (7.7)	35.6 (7.6)	2.2 (0.6)	32.2 (11.6)	25.9 (9.0)	4.1 (1.5)
17	-	-	0.0	0.00	13.9 (13.9)	65.8 (15.1)	11.1 (4.4)	0.1 (0.1)	0.1 (0.1)	23.4 (11.5)
18	-	-	0.01 (0.01)	0.00	5.2	51.9 (6.5)	12.5 (4.1)	32.0 (5.0)	0.2 (0.2)	3.3 (1.9)
19	-	2.03	0.43 (0.28)	0.00	16.2 (2.2)	-	-	-	-	-
20	-	-	0.06 (0.03)	0.04 (0.02)	6.1 (1.3)	-	-	-	-	-

Table 3: Aboveground biomass (g C m^{-2}) at each site in the Y4 watershed. Total aboveground biomass is the sum of the larch, understory vascular, standing dead tree, and woody debris biomass. Understory vascular biomass does not include lichen and moss. Values in parenthesis are standard error of the mean.

Site Number	Larch	Understory vascular	Shrub	Standing dead tree	Woody debris	Total live	Total dead	Total Aboveground
1	392 (313)	112 (41)	52 (52)	0 (0)	322 (87)	504 (304)	322 (87)	826 (389)
2	603 (244)	140 (50)	75 (40)	0 (0)	76 (7)	744 (213)	76 (7)	820 (217)
3	743 (125)	320 (106)	209 (146)	0 (0)	86 (15)	1063 (230)	86 (15)	1149 (235)
4	67 (66)	611 (166)	529 (176)	0 (0)	59 (17)	679 (153)	59 (17)	737 (167)
5	1362 (516)	193 (27)	96 (32)	219 (96)	122 (28)	1555 (490)	341 (105)	1896 (579)
6	1340 (635)	257 (81)	146 (69)	386 (236)	131 (50)	1597 (560)	517 (218)	2114 (361)
7	263 (65)	271 (86)	209 (73)	0 (0)	24 (8)	533 (45)	24 (8)	557 (52)
8	471 (303)	170 (115)	124 (108)	27 (27)	10 (3)	641 (294)	37 (29)	678 (319)
9	122 (68)	176 (93)	64 (35)	0 (0)	37 (11)	298 (60)	37 (11)	335 (65)
10	697 (405)	183 (64)	51 (51)	262 (140)	106 (16)	880 (400)	368 (153)	1248 (501)
11	227 (201)	185 (87)	95 (95)	0 (0)	62 (17)	413 (285)	62 (17)	475 (278)
12	6 (6)	116 (39)	22 (13)	0 (0)	18 (4)	122 (45)	18 (4)	140 (45)
13	698 (124)	139 (25)	32 (18)	93 (69)	306 (189)	837 (126)	399 (146)	1236 (217)
14	5 (4)	253 (184)	169 (152)	0 (0)	16 (2)	259 (183)	16 (2)	275 (181)
15	142 (85)	180 (41)	82 (48)	0 (0)	71 (63)	322 (59)	71 (63)	393 (6)
16	984 (491)	470 (256)	417 (261)	0 (0)	56 (21)	1454 (628)	56 (21)	1510 (633)
17	0 (0)	2657 (2575)	2621 (2588)	0 (0)	118 (72)	2657 (2575)	118 (72)	2775 (2642)
18	2 (2)	263 (46)	245 (42)	0 (0)	16 (5)	265 (47)	16 (5)	281 (50)
19	35 (21)	465 (172)	382 (177)	0 (0)	116 (45)	500 (159)	116 (45)	615 (196)
20	585 (217)	321 (163)	156 (105)	47 (26)	158 (140)	906 (173)	205 (118)	1111 (244)

851

Table 4: Soil carbon in the Y4 watershed. Thawed soil cores were sampled from 6 locations per site. Permafrost cores were sampled to 1 m at 7 sites (3/site). Root C and soil C values were normalized to 10 cm. The combined soil C value is the amount of C in the top 10 cm of soil, regardless of soil type (mineral/organic). Carbon pools from the permafrost cores include active layer soil (0-30 or 0-100 cm from top of ground surface). Values in parenthesis are standard error of the mean.

Site Number	Thawed Soil Cores					Permafrost Cores	
	Root C (g C m^{-2})		Soil C (kg C m^{-2})			C in top 30 cm (kg C m^{-3})	C in top 100 cm (kg C m^{-3})
	Organic	Mineral	Organic	Mineral	Combined		
1	137 (27)	0	2.60 (0.27)	2.03 (0.21)	2.34 (0.22)	4.69 (0.06)	9.36 (0.09)
2	97 (60)	0	1.35 (0.11)	1.46 (0.32)	1.32 (0.12)	3.67 (0.34)	10.16 (0.60)
3	108 (42)	0	1.86 (0.32)	1.43 (0.19)	1.83 (0.29)		
4	169 (183)	0	2.06 (0.47)	2.06 (0.22)	2.49 (0.48)		
5	453 (108)	0	4.47 (1.74)	1.57 (0.05)	3.42 (0.76)		
6	230 (169)	0	3.86 (1.03)	2.22 (0.43)	3.71 (0.93)		
7	44 (22)	0	1.13 (0.22)	2.31 (0.41)	1.14 (0.22)	4.29 (0.32)	10.48 (0.67)
8	69 (25)	0	1.25 (0.12)	2.79 (0.67)	1.38 (0.19)		
9	177 (17)	45 (31)	2.51 (0.26)	1.54 (0.33)	2.41 (0.40)	4.85 (0.36)	8.63 (0.71)
10	278 (35)	0	2.12 (0.45)	1.36 (0.12)	2.10 (0.46)	4.82 (0.44)	9.39 (0.06)
11	520 (346)	6 (4)	1.63 (0.42)	2.02 (0.16)	1.66 (0.30)		
12	271 (87)	0	1.39 (0.04)	3.26 (0.83)	1.51 (0.05)		
13	267 (30)	0	1.65 (0.28)	1.96 (0.29)	1.66 (0.29)		
14	252 (74)	6 (4)	3.12 (0.47)	1.31 (0.26)	2.74 (0.15)		
15	103 (8)	0	2.04 (0.58)	2.15 (0.53)	1.84 (0.38)		
16	189 (184)	20 (11)	1.70 (0.57)	2.08 (0.49)	1.66 (0.33)	5.32 (1.19)	11.90 (3.83)
17	0	97 (35)	-	2.37 (0.21)	2.76 (0.78)		
18	95 (36)	0	2.19 (0.40)	2.66 (2.21)	1.49 (0.55)		
19	205 (91)	203 (152)	3.51 (0.47)	2.74 (1.23)	2.85 (0.72)		
20	0	0	2.44 (0.70)	1.41 (0.26)	1.85 (0.43)	5.70 (0.55)	11.91 (0.90)

Table 5: Properties of thawed soil in the Y4 watershed. The mineral layer was collected to approximately 10 cm below the organic layer (see methods). No relationship existed between sample date and thaw depth or sample date and water content. Values in parenthesis are standard error.

Site Number	Thaw depth (cm)	Organic Layer Depth (cm)	Bulk Density (g cm^{-3})		Gravimetric Water Content (%)		Carbon Content (%)	
			Organic	Mineral	Organic	Mineral	Organic	Mineral
1	23 (1)	13 (1)	0.078 (0.021)	0.52 (0.16)	198.9 (34.4)	64.7 (17.4)	37.6 (3.5)	6.9 (2.5)
2	22 (1)	11 (1)	0.040 (0.011)	0.64 (0.05)	203.8 (28.0)	33.9 (5.8)	38.3 (4.1)	2.4 (0.5)
3	24 (1)	14 (1)	0.062 (0.011)	0.70 (0.11)	103.3 (16.2)	29.1 (4.4)	30.4 (2.2)	2.3 (0.6)
4	41 (2)	10 (1)	0.148 (0.063)	0.54 (0.14)	107.3 (28.9)	61.0 (15.6)	26.6 (4.0)	8.7 (3.0)
5	23 (1)	8 (1)	0.120 (0.032)	1.02 (0.08)	220.2 (23.1)	25.6 (2.1)	39.2 (3.2)	1.6 (0.3)
6	21 (2)	9 (1)	0.113 (0.039)	0.63 (0.05)	182.0 (19.8)	34.2 (6.1)	39.0 (3.0)	3.8 (1.0)
7	21 (1)	12 (1)	0.026 (0.005)	0.76 (0.18)	348.5 (48.4)	43.6 (10.2)	44.4 (2.0)	3.9 (1.2)
8	16 (1)	11 (1)	0.027 (0.002)	0.68 (0.10)	304.9 (32.1)	46.4 (10.3)	46.7 (0.6)	4.4 (1.1)
9	26 (2)	13 (1)	0.082 (0.010)	0.64 (0.12)	171.3 (29.5)	46.5 (11.2)	30.9 (4.4)	5.5 (2.1)
10	23 (1)	11 (1)	0.048 (0.007)	0.89 (0.05)	272.6 (15.2)	26.5 (1.7)	43.6 (1.9)	1.6 (0.2)
11	35 (2)	10 (1)	0.060 (0.023)	0.84 (0.12)	142.8 (17.8)	39.4 (6.9)	30.5 (3.3)	3.6 (1.6)
12	29 (2)	10 (1)	0.053 (0.020)	0.67 (0.10)	247.7 (17.5)	58.3 (10.7)	43.5 (1.8)	5.0 (1.0)
13	29 (1)	12 (1)	0.042 (0.008)	0.71 (0.11)	194.1 (15.4)	48.6 (12.6)	40.0 (1.4)	4.0 (1.0)
14	42 (2)	8 (1)	0.103 (0.016)	0.82 (0.10)	165.8 (14.7)	31.0 (7.2)	32.4 (3.8)	3.0 (1.6)
15	28 (2)	12 (1)	0.150 (0.099)	0.92 (0.10)	419.1 (105.4)	39.9 (10.6)	38.3 (3.5)	2.6 (0.9)
16	24 (1)	12 (1)	0.042 (0.009)	0.76 (0.18)	256.3 (38.8)	49.5 (15.8)	40.2 (2.1)	5.9 (3.4)
17	45 (2)	9 (2)	-	0.46 (0.11)	-	50.9 (7.6)	-	8.7 (2.8)
18	26 (1)	18 (1)	0.059 (0.012)	0.39 (0.20)	346.8 (45.4)	123.2 (31.2)	39.9 (3.3)	8.7 (2.6)
19	36 (2)	14 (2)	0.078 (0.022)	1.40 (0.09)	204.9 (52.3)	22.8 (0.4)	33.5 (3.4)	1.0 (0.1)
20	29 (1)	9 (1)	0.118 (0.001)	0.65 (0.31)	252.9 (76.6)	76.1 (28.4)	29.9 (4.4)	8.6 (4.9)

Figure 1

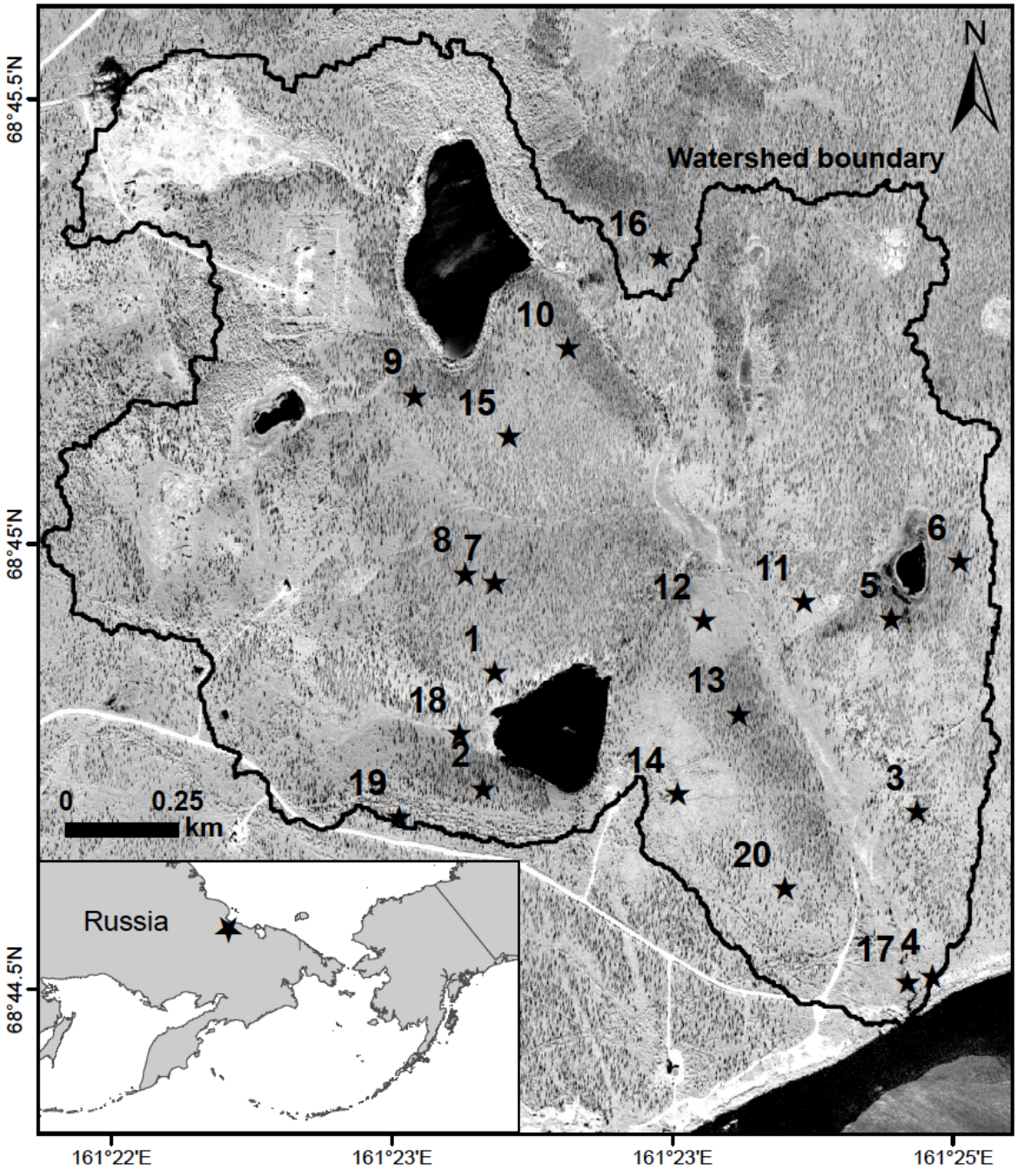
N
Watershed boundary
16
10
9
15
8
7
6
11
12
5
1
13
18
2
14
3
19
20
17
4
0
0.25
km
Russia
68°45.5'N
68°45'N
68°44.5'N
161°22'E
161°23'E
161°23'E
161°25'E

Figure 2

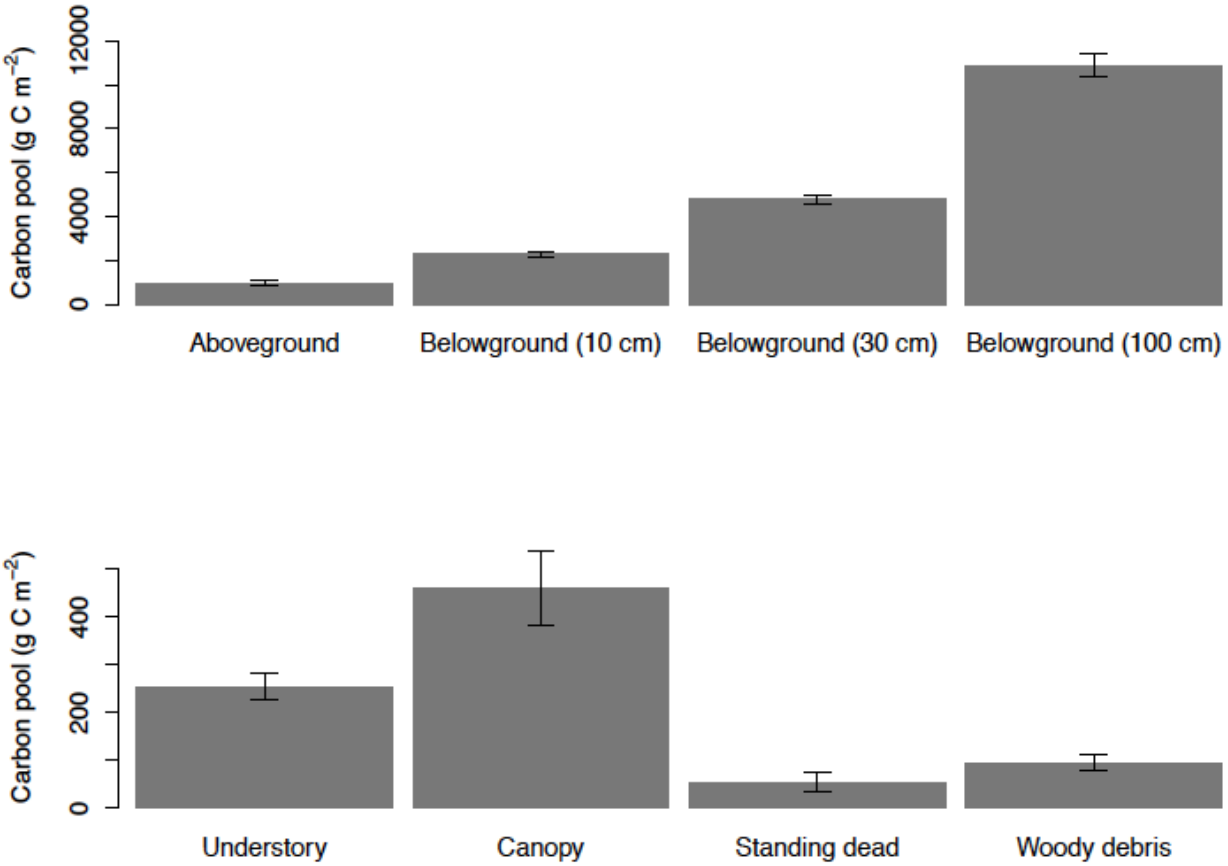
Carbon pool (g C m^{-2})
0
4000
8000
12000
Aboveground
Belowground (10 cm)
Belowground (30 cm)
Belowground (100 cm)
Carbon pool (g C m^{-2})
0
200
400
Understory
Canopy
Standing dead
Woody debris

Figure 3

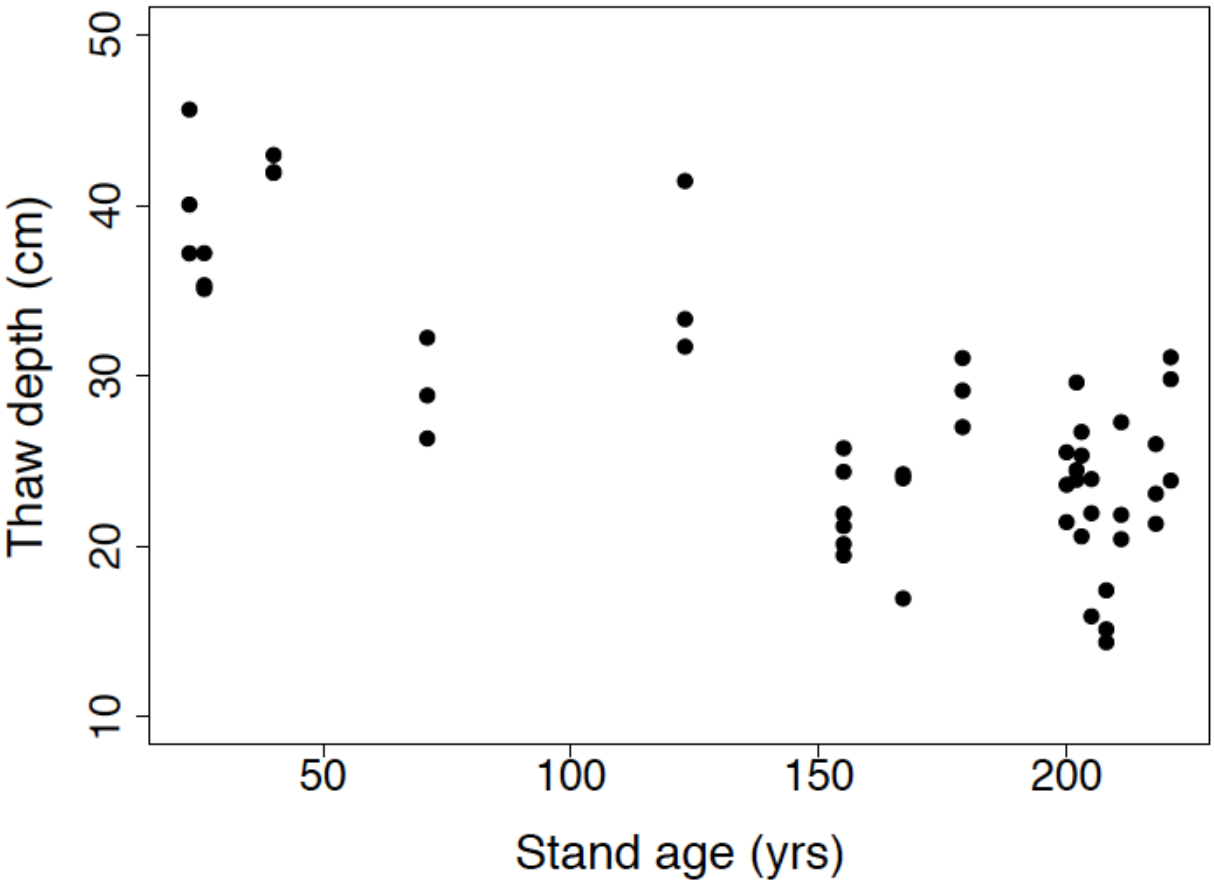

Figure 4

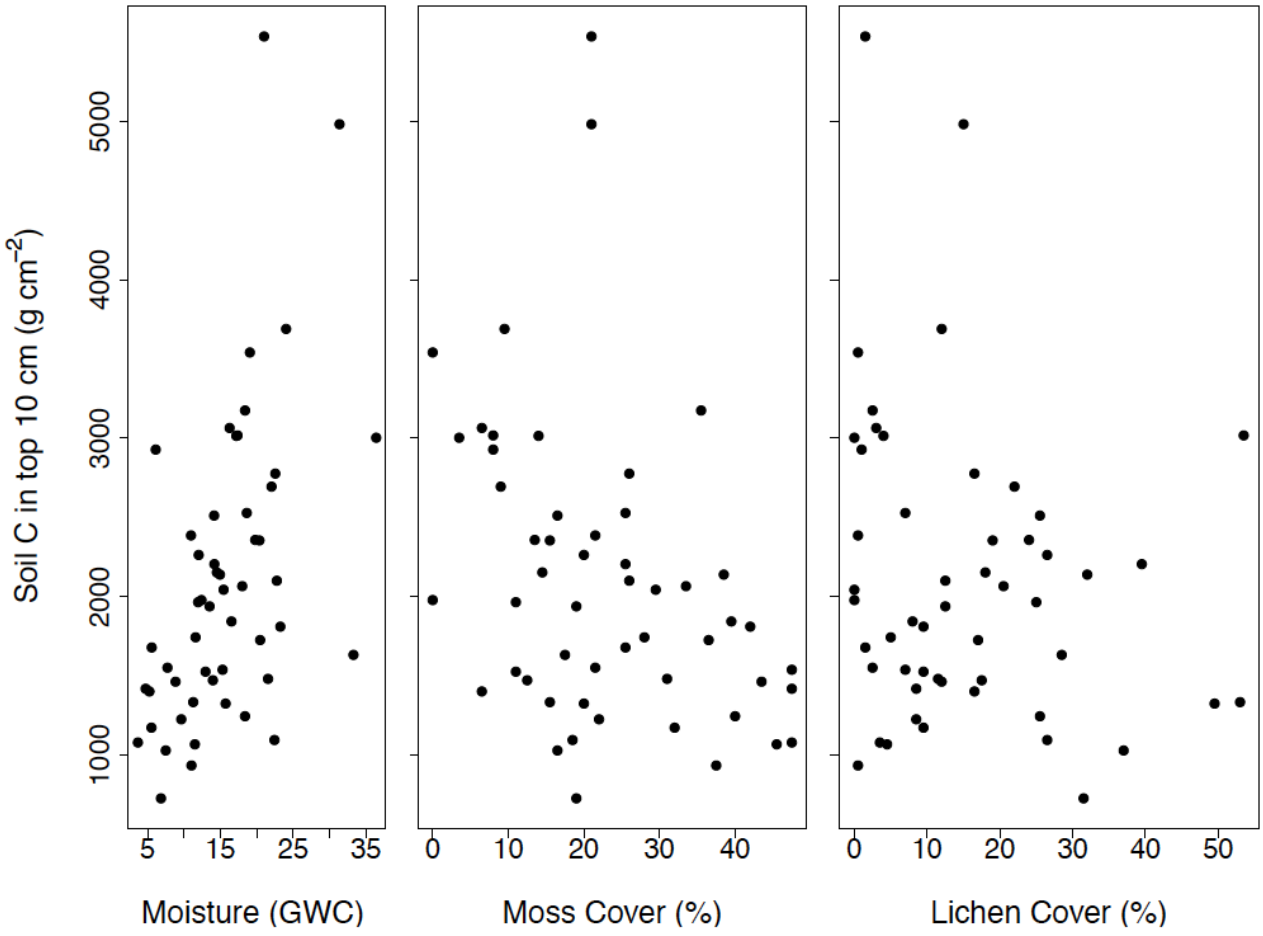
Soil C in top 10 cm (g cm^{-2})
1000
2000
3000
4000
5000
5
15
25
35
Moisture (GWC)
0
10
20
30
40
Moss Cover (%)
0
10
20
30
40
50
Lichen Cover (%)

Figure 5

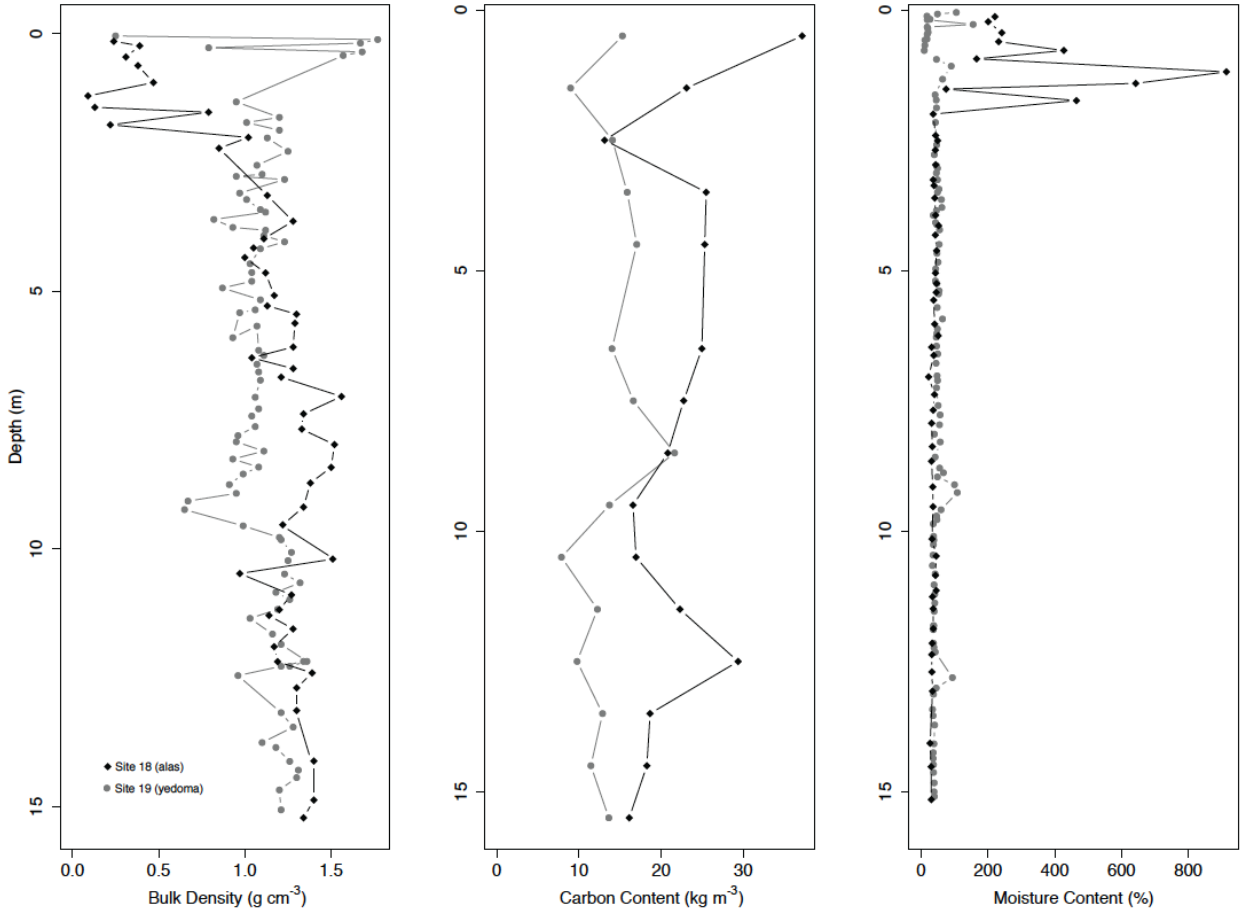
Depth (m)
0
5
10
15
0.0
0.5
1.0
1.5
Bulk Density (g cm-3)
Site 18 (alas)
Site 19 (yedoma)
0
10
20
30
Carbon Content (kg m-3)
0
200
400
600
800
Moisture Content (%)